ENN Encyclopedia of Nanoscience and Nanotechnology
www.aspbs.com/enn

Self-Assembled Nanofibers

Hirotaka Ihara, Makoto Takafuji, Toshihiko Sakurai

Kumamoto University, Kumamoto, Japan

CONTENTS

1. INTRODUCTION

This article introduces nanofibrillar structures created by self-assembling. The term "self-assembled nanofibers" refers to strands with various shapes such as helices, ribbons, and tubes. Biological organisms are constructed by molecular building blocks and these molecules are assembled spontaneously through various intermolecular interactions [1–6]. Life itself is hierarchically composed of self-assembling molecular building blocks.

There are many kinds of assembled nanofibers in nature. DNA is a double-stranded molecule [7–11]. Each spiraling strand, comprised of a sugar-phosphate backbone and attached bases, is connected to a complementary strand by noncovalent hydrogen bondings between paired bases. Actin forms twisted, rope-like filaments known as F-actins, which are made up of identical building blocks called G-actin subunits [12–14]. Tobacco mosaic virus, for example, forms 300 nm in length × 18 nm in diameter rod-like assemblies composed of 2130 identical protein-armored cylindrical RNAs [15–19]. Each protein subunit contains 158 amino acids.

On the other hand, many artificially self-assembled nanofibers have also been reported in the last two decades [20–32]. Various aggregation morphologies such as helices, tubes, fibers, and ribbon-like and rod-like morphologies have been identified by optical, electron, and probe microscopic observations. Most of their root compounds were serendipitously discovered to form self-assembled nanofibers [33]. The morphologies and properties of these molecular assemblies have attracted the interest of many researchers in a wide range of research fields.

The self-assembled nanofibers themselves can be obtained by simple preparation methods—for instance, by dispersing compounds into media by heat or sonication and then allowing them to stand at a given temperature for a few minutes to several days. These self-assembled nanofibers are interesting due to their numerous potential applications and for understanding biological systems.

Now it is possible to select from a large number of molecular models because many synthetic compounds have been found to form self-assembling nanofibers as well as biomolecules. In this article, the authors would like to introduce self-assembled nanofibrillar aggregates, and specific attention will be paid to aqueous bilayer membrane systems and organogel systems. These self-assemblies show not only unique morphologies but also high molecular orientation toward special functions, for which molecular chirality is an especially important factor. Mirror images of morphologies are formed from enantiomer, and racemates will often destroy developed aggregates [34, 35]. This suggests that chirality is not unrelated with the evolution of life. Well-designed, self-assembled nanofibers can support nanoscopic technologies and their applications.

2. NANOFIBERS FROM COVALENT SYSTEMS

Carbon nanotubes were first discovered in 1991 by S. Iijima et al. as a by-product, while they were examining the generation mechanism of fullerene [36, 37]. These carbon nanotubes form a graphite structure made of a net-like carbon surface in the shape of a cylinder, and both single-wall carbon nanotubes (SWNT) (Fig. 1a) [38, 39], consisting of a single graphitic carbon sheet, and multi-wall carbon nanotubes (MWNT) (Fig. 1b) [37] with a multi-wall structure have been confirmed. The diameter of the single-wall nanotubes is 3 nm and its central cavity is 1–2 nm. On the other hand, the diameter of multi-wall nanotubes ranges from 5–50 nm and the outer diameter of the central cavity can be from 3–10 nm. Characteristically, their lengths exceed 10 μm and both types have a high aspect ratio in every direction. Until now, they were considered expensive solid

ISBN: 1-58883-065-9/$35.00

Encyclopedia of Nanoscience and Nanotechnology
Edited by H. S. Nalwa
Volume 9: Pages (473–495)

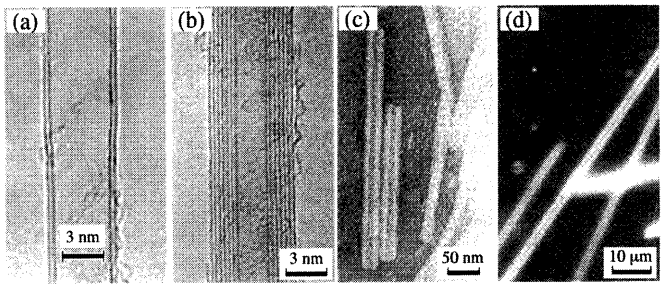

Figure 1. (a) Single-wall and (b) multiwall carbon nanotubes [36–38], and (c) single-wall organic nanotube [21] and (d) organic microtube from synthetic lipids [43]. Reprinted with permission from [36], S. Iijima, *Nature* 354, 56 (1991). © 1991, from [21], K. Yamada et al., *Chem. Lett.* 1713 (1984). © 1984, The Chemical Society of Japan; and from [43], N. Nakashima et al., *J. Am. Chem. Soc.* 107, 509 (1985). © 1985, American Chemical Society.

carbon compounds as their yield was low. Presently, however, these materials can be created relatively cheap using new industrial methods [40, 41] including discharge, laser evaporation, and catalyst chemical vapor deposition methods, and their application in various fields is being actively explored.

On the other hand, the history of organonanotubes produced from organic matter is much older. In 1984, one of the present authors confirmed that one polypeptide lipid formed aggregates in the shape of a tube with an inner diameter of 4–10 nm and a length of 50–200 nm by self-assembly in an aqueous solution (Fig. 1c) [21]. Since the width of the wall was approximately 5 nm, it is presumed to have been formed as a single-wall bilayer. Nanotubes from longer single-wall bilayers have also been reported in subsequent research [24, 31, 32]. Nakashima et al. discussed microtubes (Fig. 1d) based on bilayer structures [42, 43].

In 2001, *Science* chose carbon nanotubes as one of the top 10 research domains, and growing interest in nanotubes from the field of molecular device physics indicates their application potential in the electronics industry of the future. Especially, SWNTs of approximately 1 nm in diameter have been shown theoretically [44–49] and experimentally [50–53] to become both metal-like and semiconductor-like, and the production and operation of transistors using carbon nanotubes has been reported [54].

Research has already begun on the electronic characteristics of hybrid structures created by inserting different molecules into the space in the center of a nanotube. Iijima and Smith et al. have reported one-dimensional crystallization of C60 molecules by Van der Waals interaction formed by introducing fullerene into nanospace through the deficit part of SWNT and annealing it [55–57]. Further tests have been performed by inserting Ga encapsulated fullerene (Ga@C82) into the SWNT instead of C60, and these results also showed the formation of structures crystallized in one dimension by regular intervals like C60 (Fig. 2a) [57]. On the other hand, similar encapsulation behavior can be attained by organic nanotube systems. Shimizu has excellent photographs of vesicle-encapsulated nanotubes (Fig. 2b) [58].

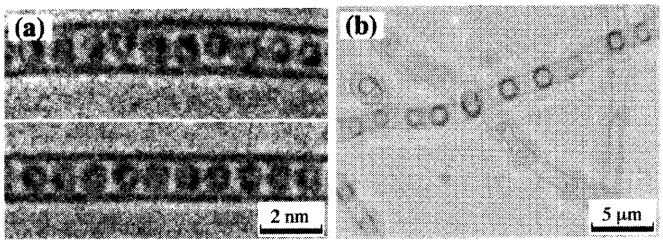

Figure 2. TEM images of (a) carbon nanotube encapsulated Ga@C82 [57] and (b) organic nanotubes encapsulated vesicles [58]. Reprinted with permission from [57], S. Iijima, *Physica* B 323, 1 (2002). © 2002, Elsevier Science; and from [58], T. Shimizu, *Macromol. Rapid Commun.* 23, 311 (2002). © 2002, Wiley-VCH.

In contrast to organonanotubes, carbon nanotubes have an essential characteristic property of high electroconductivity, as well as a stable chemistry structure and a morphology that can be kept stable as well. For these reasons, these nanomaterials are certain to be very important in future nanotechnology [54, 59–62]. However, conversely, only limited chemical modification can be performed and addition or conversion of functions is not easy. Self-assembling organotubes, on the other hand, are admittedly unstable both physically and chemically, but the molecules that form them can be exchanged by taking advantage of their aggregate feature, allowing them to take on many different kinds of functions. Moreover, morphologically, they do not necessarily generate tubes alone—various nanofibrillar aggregate morphologies are possible, among which the tube-like aggregate is simply comparatively one of the most stable. This section will end with a brief description of the names of various morphologies that have been produced by self-assembly until now (Fig. 3).

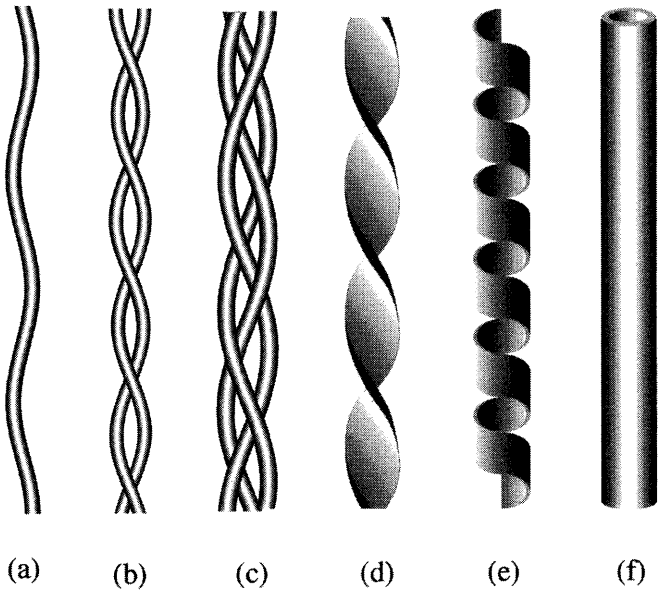

Figure 3. Classification of nanofibrillar aggregates. (a) rope-like fibril, (b–c) multistrand fibril, (d) twisted ribbon-like fibril, (e) helical ribbon-like fibril, and (f) tubular fibril.

3. NANOFIBERS FROM NONCOVALENT SYSTEMS

3.1. Characterization

Self-assembled nanofibers are generally prepared by dispersing into aqueous or nonaqueous (organic solvents) media with heating and sonication procedures, and then allow to stand the solution at designated temperature for few minutes to several days. Some cases are accompanied by macroscopic transformations through formation of well-developed aggregates. A typical example is a viscosity increase and, thus, the judgment of gelation of organic solvents are conventionally carried out by an inversion fluid method [63].

Microscopic techniques are useful for observation of aggregation morphologies—optical microscopes and scanning and transmission electron microscopes (SEM and TEM). Typical examples will be shown in Figures 1, 2, 5, 8, and 13. Scanning probe microscopes such as atomic force microscope (AFM) have also been used to obtain detailed information on the self-assembled morphologies. Figure 4 shows typical AFM images of the lithosatahine protofibriles [64]. A large number of photographs and images of self-assembled aggregates show various fiber-like morphologies such as rods, tubes, helices, ribbons, tapes, and twisted multiple strands. The freeze-fracture and freeze-drying techniques can be combined with these microscopic observations. Small-angle X-ray scattering (SAXS) and small-angle neutron scattering (SANS) are important techniques to obtain the information of practical quantities such as diameter, thickness, and length of aggregates. Figure 5 shows an example of the powder X-ray diffraction (XRD) spectra of zerogels prepared by freeze-drying of fibrillar aggregate-containing organogels. The authors discussed the molecular packing mode [65]. Thermodynamic properties are, in most cases, performed by differential scanning calorimeter (DSC) [66–73]. Most self-assembled aggregates show phase-transition phenomena such as gel (crystal)-to-liquid crystal and gel (crystal)-to-sol, and thus physicochemical properties of the aggregates drastically change at their transition temperatures. Spectroscopic observations provide information on molecular orientations, packing states, and lateral diffusion behavior. UV-visible [32, 69, 73–76], Fourier transform infrared (FT-IR), circular dichroism (CD) [21, 22, 32, 73, 76–78], fluorescence [79, 80], and nuclear magnetic resonance (NMR) [81] spectrometers have been widely used for investigation and analysis on the molecular orientation. Typical investigations are found in chromophore-containing lipid systems. Shimomura et al. discussed on H- or J-aggregations with λ_{max}-shift of a UV-visible spectra [82]. Ihara et al. discussed chiral-stacking behavior among the sorbyl groups of lipids with both UV-visible and CD spectra [32]. They also discussed the photo-induced polymerization process by following the spectral changes. Hachisako et al. discussed the critical aggregation concentration with visible spectral change induced by the isomerization of the spiropiran-containing lipid [83]. Schnur et al. discussed the relationship between the molecular chirality of lipids and the helicity of aggregation morphology with CD spectra [84]. These suprastructural aggregates often provide specific binding behavior for guest molecules such as dyes. These phenomena can also be detected by UV-visible and CD spectra [76, 85–87]. Fluorescence spectra are helpful for knowing the microenvironment around lipids. Sagawa et al. reported excimer formation when a pyrenyl group-containing lipid forms highly ordered aggregates in organic solvents [80]. These typical spectral data are shown in Figures 6 and 12.

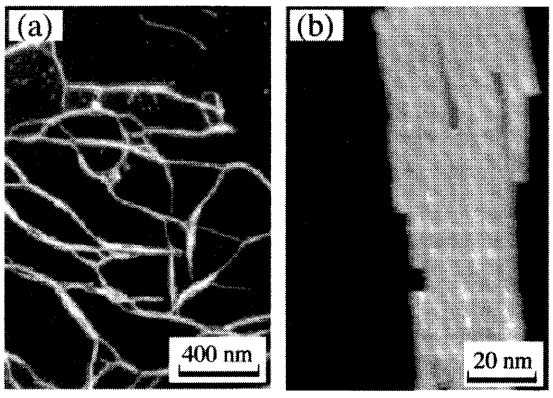

Figure 4. Morphological characterization of lithostathine protofibrils by tapping mode AFM in air (a), and in solution (b).

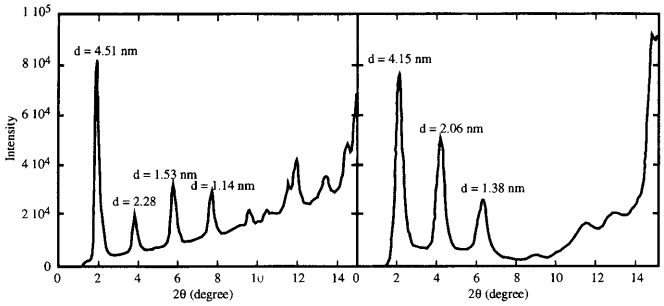

Figure 5. Powder XRD spectra of xerogels prepared from neat gels with the azobenzene-containing cholesterol derivatives [65]. Reprinted with permission from [65], J. H. Jung and S. Shinkai, *Journal of Inclusion Phenomena and Macrocyclic Chemistry* 41, 53 (2001). © 2001, Kluwer Academic Publishers.

3.2. Nanofibers in Aqueous Systems

Bio-membranes are spontaneously organized from many kinds of molecules such as phospholipids, proteins and polysaccharides. Some phospholipids (**N-1** ~ **N-4**) listed in Figure 7, which are representative of amphiphiles, form bilayer membrane structures spontaneously in water and their hydrophobicity is a major driving force in the aggregation and maintenance of the bilayer structures. These lipids usually form small globules and vesicles in water. A typical example is the vesicular structures observed when soybean-derived phosphatidyl choline is dispersed in water, which was reported in 1965 [88].

In 1977, Kunitake et al. reported in a landmark study that didodecyldimetylammonium bromide, as a totally synthetic lipid, could form bilayer structures in water [33]. Since this turning point, a large number of double-chain alkyl amphiphiles have been synthesized and characterized by many researchers. These findings led to the next step of lipid chemistry. Nobody doubts that the number of alkyl

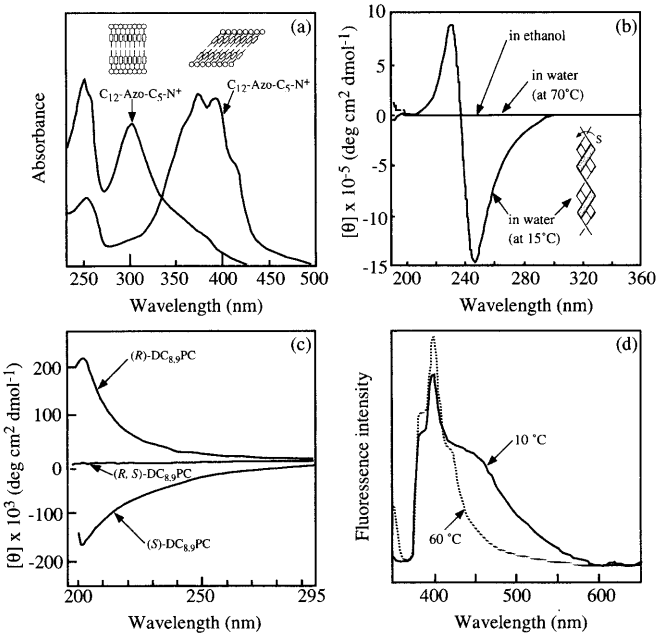

Figure 6. Typical spectral data for self-assembled nanofibers: (a) UV-visible spectra of the azobenzene-containing single alkyl-chain lipid in aqueous solution systems [82]; (b) CD spectra of the sorbyl group containing double chain-alkyl lipid in aqueous solution systems [32]; (c) CD spectra of 1,2-bis(tricosa-10,12-diynoyl)-sn-glycero-3-phosphocholines in aqueous solution systems [84]; (d) fluorescence spectra of the pyrene-containing double alkyl-chain lipid in organic solvent systems [80]. Reprinted with permission from [82], M. Shimomura et al., *Ber. Bunsenges. Phys. Chem.* 87, 1134 (1983). © 1983, Wiley VCH; from [32], H. Ihara et al., *Langmuir* 8, 1548 (1992). © 1992, American Chemical Society; from [84], J. M. Schnur et al., *Science* 264, 945 (1994). © 1994, American Association for the Advancement of Science; and from [80]. T. Sagawa et al., *Langmuir* 18, 7223 (2002). © 2002, American Chemical Society.

chains in a hydrophobic part is not directly related whether or not a lipid can form bilayer structures but its molecular shape and intermolecular interaction are rather important.

It has been recognized that bilayer membrane structures can be formed from single chains [20, 89], triple chains [90], and others [29]. Also a hydrophilic part is not within the specified structure. It has been reported forming bilayer membrane structures from amphiphiles with anionic and nonionic groups, as well as twitter ionic and cationic groups.

Through these investigations, in 1984, one of the authors found that special synthetic lipids (**B-1a**) with hydrophilic oligopeptide head groups can form helical or tubular structures in water (Figs. 8a and 8e) [21]. This finding is significant in light of the fact that the thickness of the aggregates corresponds to that of single-walled bilayer structures and that the tubular and helical forms are closely related. At the same time this report on similar tubes through lipid aggregation was published, Nakashima et al. reported that helical ribbon-like aggregates could be produced from L-glutamate-derived lipids but that these were much larger—in microsize rather than nanosize [42, 43]. Further investigation made it clear that the helical form was rather an intermediate to the tubular form and that the formation of fibrillar structures with helices and tubules is deeply related to their chiral properties [22, 24, 31].

Since 1984, many researchers have designed and synthesized chiral lipids that produce nanofibrillar structures in water. They can be roughly classified into two categories: (1) micellar-based aggregates, and (2) bilayer sheet-based aggregates. Figure 7 includes the chemical structures of synthetic lipids that can form nanofibrillar aggregates in water.

3.2.1. Micellar-Based Fibrillar Aggregates

It may be difficult to define a micellar system, but one well-known case of micellar-based aggregates from *N*-alkyl aldonamides (**B-6**) and a series of diastereomeric and enantiomeric *N*-octylaldonamides has been studied by Fuhrhop et al. since 1987 [91]. Their TEM microscopic observations indicated that the solubilities and aggregation morphologies of aldonamides depended directly on the stereochemistry of their polyol head groups (Fig. 8g). All antichain head groups, like D-Man for instance, of *N*-octylaldonamides-induced formation of sheet-like aggregates based on bilayer structures, and highly irregular chain (i.e., twisted chain) conformations, like D-Alt and D-Ido for instance, induced high water solubility with no consequent aggregation. On the contrary, cylindrical micellar aggregates were obtained from *N*-octylaldonamide with L-Glu, D-Glu, and D-Tal head groups. It was estimated that a moderate molecular bending at the head group induced high curvature in the aggregates. They proposed a model of fibrillar (cylindrical) micelles and then this arrangement was supported by ^{1}H-NMR spectroscopic measurements [92]. Furthermore, it was confirmed by detailed TEM observations and image-processing that micellar fibrils often produced multihelices by twisting themselves. *N*-Octyl and *N*-dodecyl-D-gluconamides formed self-organized quadruple helices with magic angles whose pitch is equal to $2\pi\times$ molecular bilayer diameter. Figure 8h shows its TEM image and a contour line diagram obtained by image analysis [93]. Here, each micellar fibril preserved its independence without fusion. A computer model of quadruple micellar fibrils is also shown in Figure 9.

In 1992, Imae et al. [94] reported that *N*-acyl amino acids formed fibrillar, distorted fibrillar, or twisted ribbon-like aggregates (Fig. 8i), and their aggregation morphologies were dependant upon the types of amino acids and pH of aqueous solutions. Transmission electron microscopic observations showed that *N*-dodecyl-L-aspartic acid and *N*-dodecyl-L-alanine formed distorted fibers (pH = 3.6–5.5, temperature < 12 °C) and cylindrical structures without distortion (pH < 6.0, ambient temperature), respectively. Since *N*-dodecyl-L-glutamic acid formed globular aggregates, it was estimated that the bulkiness of the head group may have influenced the aggregation morphologies. Similar micellar formation was observed in poly(amino acid)s with terminal dialkyl groups. Their aggregation morphology is influenced by the pH-dependant secondary structures of poly(amino acid)s as head groups (**B-1, 2, 3**). [22, 30, 31] The complex **B-9** is known as bolaamphiphiles, which form spherical micelles or vesicles in aqueous solutions as well as amphiphiles. **B-9** is an asymmetric bolaamphiphile with one amino acid head group and one ammonium chloride head group. The diameter of their fibers is 2.5 nm, which corresponds exactly to that of micellar monolayers. (Fig. 8j) [58].

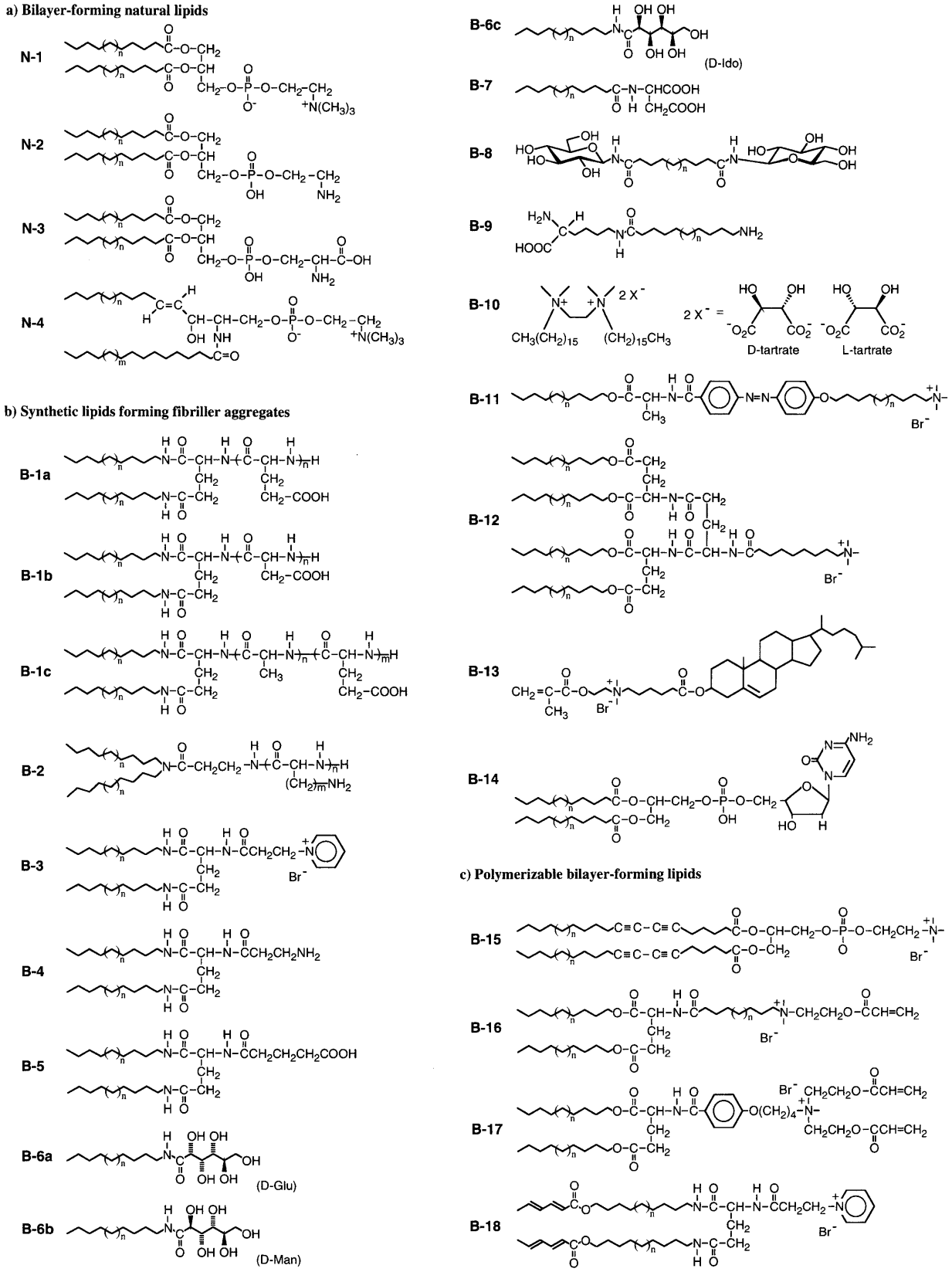

Figure 7. Chemical structures of aqueous bilayer membrane-forming chiral lipids (Ref.: **B-1a** [21, 24], **B-1b** [22, 24], **B-1c** [31], **B-2** [24], **B-3** [30], **B-4** [76], **B-5** [170], **B-6** [91, 92], **B-7** [94], **B-8** [58], **B-9** [94], **B-10** [95, 96], **B-11** [74], **B-12** [29], **B-13** [26], **B-14** [28], **B-15** [25], **B-16** [103], **B-17** [103], **B-18** [32]).

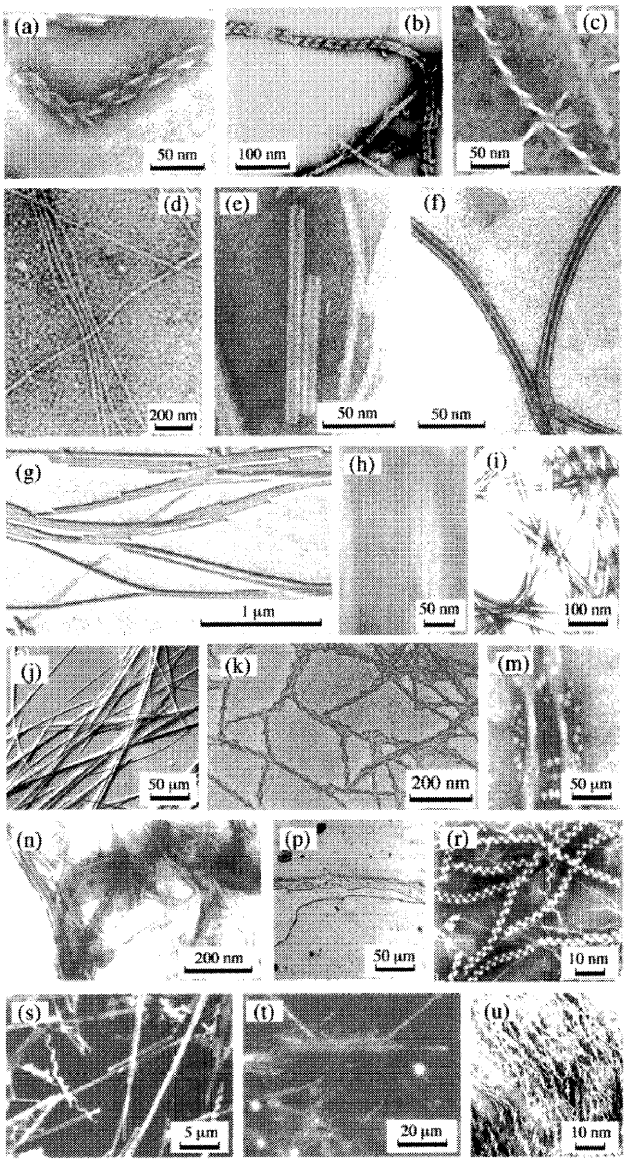

Figure 8. Various nanofibrillar aggregates from aqueous lipid membrane systems. (a) **B-1a** [21], (b) **B-3**, (c) **B-3** [30], (d) **B-1b** [22], (e) **B-1a** [21], (f) **B-3** [30], (g) D-talonamide derivative [27], (h) *N*-octyl-D-gluconamide [93], (i) *N*-dodecanoyl-β-alanine [94], (j) bolaamphiphile [58], (k) **B-10** [95], (m) **B-10** [96], (n) **B-12** [29], (p) **B-13** [26], (r) **B-14** [28], (s) **B-15** [25], (t) **B-16** [103], (u) **B-18** [32]). Reprinted with permission from [21], K. Yamada et al., *Chem. Lett.* 1713 (1984). © 1984, The Chemical Society of Japan; from [30], H. Ihara et al., *J. Chem. Soc. Jpn.* 1047 (1990). © 1990, The Chemical Society of Japan; from [27], J.-H. Fuhrhop et al., *J. Am. Chem. Soc.* 110, 2861 (1988). © 1988, American Chemical Society; from [93], J. Koning et al., *J. Am. Chem. Soc.* 115, 693 (1993). © 1993, American Chemical Society; from [94], T. Imae et al., *J. Am. Chem. Soc.* 114, 3414 (1992). © 1992, American Chemical Society; from [58], T. Shimizu, *Macromol. Rapid Commun.* 23, 311 (2002). © 2002, Wiley-VCH; from [95], R. Oda et al., *Nature* 399, 566 (1999). © 1999, Macmillan Magazines Ltd; from [96], R. Oda et al., *Angew. Chem. Int. Ed.* 37, 2689 (1998). © 1998, Wiley-VCH; from [29], N. Kimizuka et al., *Chem. Lett.* 29, (1990). © 1990, The Chemical Society of Japan; from [26], I. Cho and J. G. Park, *Chem. Lett.* 977 (1987). © 1987, The Chemical Society of Japan; from [28], H. Yanagawa et al., *J. Am. Chem. Soc.* 111, 4567 (1989). © 1989, American Chemical Society; from [25], J. H. Georger et al., *J. Am. Chem. Soc.* 109, 6169 (1987). © 1987, American Chemical Society; from [103], T. Kunitake et al., *Macromolecules* 22, 3544 (1989). © 1989, American Chemical Society; and from [32], H. Ihara et al., *Langmuir* 8, 1548 (1992). © 1992, American Chemical Society.

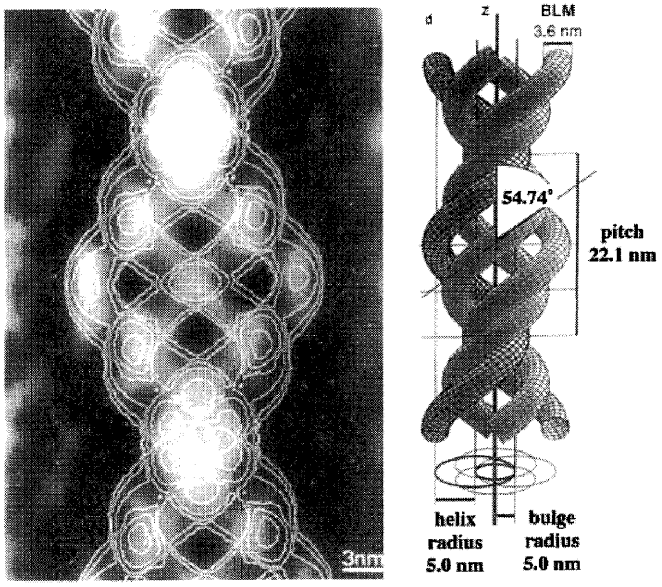

Figure 9. A computer model of quadruple micellar fibrils [93]. Reprinted with permission from [93], J. Koning et al., *J. Am. Chem. Soc.* 115, 693 (1993). © 1993, American Chemical Society.

3.2.2. Bilayer Sheet-Based Fibrillar Aggregates

So far, a large number of bilayer-forming lipids have been reported, including some that can form helical and twisted ribbon-like aggregates. Their assemblies are based on distorted sheet-like bilayer membranes with large curvature and are morphologically divided into helical and tubular structures with cylindrical curvature and twisted ribbons with Gaussian, saddle-like curvature.

The first observation was reported in 1984. Didodecyl L-glutamide derivatives with oligo(L-glutamic acid) head groups (**B-1a**) formed helical or tubular aggregates [21]. Transmission electron microscopic observations showed that the **B-1a** formed helical aggregates (Fig. 8a) immediately after dispersion and then grew to tubular aggregates (Fig. 8e). It was confirmed that the tubular aggregates were 5–6 nm thick, which corresponds to the thickness of single-layered bilayer membranes (two molecular lengths) of lipid **B-1a**, and their diameters were 20–25 nm. On the other hand, when the head group is composed of the corresponding DL-glutamic acid, only large sheets without curvature were produced [24].

In addition, when oligo(L-aspartic acid) was used instead of oligo(L-glutamic acid) as the head group of **B-1b**, fibrillar and twisted ribbon-like aggregates were formed (Fig. 8d) [22]. Through these studies, we were also able to reveal the process of morphogenesis of these suprastructural aggregates by TEM observation and light scattering measurement:

1. **B-1b** formed globular aggregates with the largest curvature at the initial step;
2. these globules grew to fibrillar aggregates;
3. double or multiple strands were produced and then fused themselves to make ribbon-like aggregates.

These findings indicate that even a very small difference between L-glutamic and L-aspartic acid in the head group strongly influences the morphology of the aggregates. This

means that aggregation morphology is also very sensitive to temperature and pH factors because these can drastically change the secondary structures of the head groups.

Oda et al. described the difference between helical (and tubular) and ribbon-like aggregates formed from charged gemini surfactants **B-10** with chiral counterions (Figs. 8k and 8m) [95, 96]. In these studies, helical aggregates were formed from long-chain (C_{18}) surfactants, whereas twisted ribbon-like aggregates were formed from short-chain (C_{14} or C_{16}) surfactants. The degree of twist and the pitch of the ribbons could be controlled by the introduction of opposite-handed chiral counterions in various proportions.

In 1985, Helfrich and Harbich [97] attempted to define a theoretical approach for the morphologies of helical and twisted aggregates. An explanation of these phenomena, Oda et al. demonstrated their own theoretical approach using the extended Helfrich model [98–100]. Other researchers have endeavored to solve a riddle of being between geometrical morphologies and chemical structures [101, 102]. So far, no consensus has been established, because supramolecular assembly-forming compounds include many different chemical structures. Several questions still remain; for instance, the nature of the edge of the bilayers has not been clarified. Future work in both experimental and theoretical studies will develop technologies for order-made self-assembling nanofibers.

Two common features necessary for the chemical structure of molecules that form supramolecular assemblies are a chiral carbon atom and moieties feasible for intermolecular interactions. Artificial chiral lipids that can form supramolecular assemblies such as helical, tubular, and ribbon-like aggregates based on bilayer membrane structures are listed in Figure 7. This includes single chain (**B-11**) [74], quadriplex chain (**B-12**) [29], and cholesterol group (**B-13**) [26] as hydrophobic part, and nucleotide group (**B-14**) [28] as a hydrophilic part. Moreover, polymerizable moieties such as diacetyrene group (**B-15**) [25], acrylate group (**B-16, 17**) [103], methacrylate (**B-13**) [26], and sorbate group (**B-18**)-containing lipids [32] have been also reported. Figure 8 includes their typical TEM images.

3.2.3. Non-Lipid Based-Nanofibers

The preceding section discussed special nanofiber structures formed by hydrophobic aggregation and by intermolecular interaction with polar groups. Here, is described the formation of nanofibrillar structures through multiple hydrogen bonding and, consequently, molecular orientation (Figure 10).

On the other hand, the construction and structural analyses of aggregates caused by β-structures are also performed from the viewpoint of protein chemistry [104–108]. For example, prion proteins from patients with Alzheimer's disease or Bovine Spongiform Encephalopathy (BSE) form a different fiber-like aggregate [109–111] than prion proteins from a healthy body, and these proteins include β-structure [112–114].

Although Scrocchi et al. did not aim to produce nanofibers, they chose an arrangement of 6 out of the 37 residues in the human islet amyloid polypeptide (hIAPP) amino acids sequence (**P-1**), and specified the sequence that

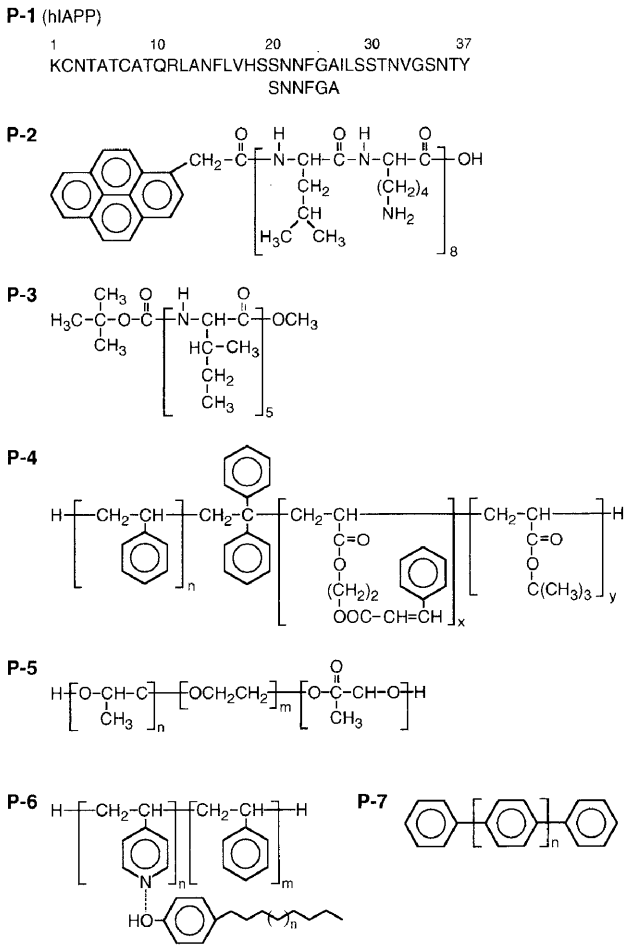

Figure 10. Chemical structures of peptides and other polymers that can form nanofibrillar aggregates (Ref.: **P-1** [109], **P-2** [115], **P-3** [111], **P-4** [192], **P-5** [191], **P-6** [187], **P-7** [198]).

makes hIAPP β-formed [109]. Consequently, it was found that the hexapeptides of hIAPP (residues 20–25) promote β-transition of IAPP most strongly, and were seen to produce nanofibers (Fig. 11a). This was especially interesting as it showed that an amino acid sequence of only six residues could serve as a trigger for proteinic β-form induction to

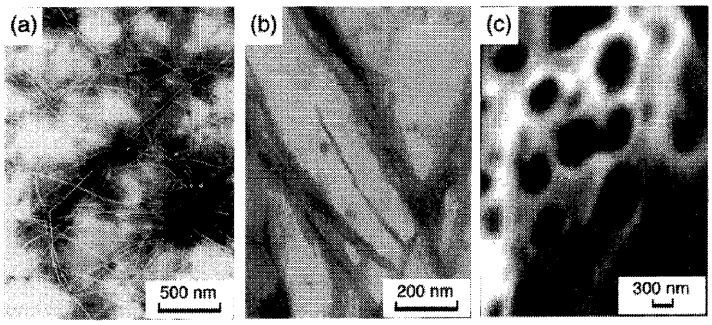

Figure 11. TEM images of (a) **P-1** fibrils after incubation with SNNFGA [109], (b) **P-2** fibrils obtained from an aqueous solution with 200 eq [115]. NaCl and (c) **P-3** aggregates formed from a chloroform solution [111]. Reprinted with permission from [109], L. A. Scrocchi et al., *J. Mol. Biol.* 318, 697 (2002), © 2002, Academic Press; from [115], T. Sakurai et al., *Chem. Lett.* (in press). ©—, The Chemical Society of Japan; and from [111], R. Jayakumar et al., *Langmuir* 16, 1489 (2000). © 2000, American Chemical Society.

form a nanofiber. However, nanofibers of β-structure origin have extremely low solubility and do not dissolve easily. Therefore, they are not suitable for use as nanostructure materials.

To overcome this hurdle, construction of water-soluble nanofibers from β-structures is now being studied [115]. We have noticed that when sequential oligopeptides with alternating hydrophilic and hydrophobic residues form β-structures, they may also be able to form amphiphilic structures. As an example, a Lys-Leu alternating sequential oligopeptide (**P-2**) was synthesized, and it was confirmed that helical tape-like aggregates were formed in the solution. Transmission electron microscopic images showed that the width of the thinnest portion was approximately 12 nm (Fig. 11b). Moreover, when fluorescence spectra of pyrenyl chromophores at the terminal end of the main chain were investigated, we found excimer formation that demonstrates orientation between the pyrenyl chromophores at the time of nanofiber formation. On the other hand, neither nanofiber formation nor excimer generation was observed in random copolypeptide.

Similar formation of aggregates from β-structures of oligopeptides (**P-3**) was reported by Jayakumar et al., who observed that L-Ileu pentapeptides form aggregates in toluene and DMF (Fig. 11c) [111]. In this case, however, they were insoluble and it was not specified whether nanofiber structure was formed.

3.2.4. Chiral Properties of Suprastructural Bilayer Membranes

Most nanofibrillar assemblies based on micells and bilayer membranes possess chiral centers in their structures. Of course, the chirality of molecules plays an important role in the production of distorted supramolecular assemblies. We have observed that oligo(L-glutamic acid)-containing lipids (**B-1a**) produce nanofibrillar aggregates including helices and tubules but that corresponding DL-derivatives produce only large sheet aggregates [24]. Similar observations have been made for other lipids (**B-6** and **10**): enantiomeric compounds form right-handed and left-handed helical aggregates, and equimolar mixtures (= racemates) often induce drastic morphological change [27, 95]. It is considered that the molecules in the distorted aggregates pack with slight angle with their neighbors, and this feature of molecular orientation produces some unique properties. **B-3** [30], in which dialkyl chains and pyridinium moieties are connected by L-glutamide through three amide groups, formed helical and tubular aggregates. Here, DSC measurement showed two endothermic peaks (with top temperatures of 33 °C (T_1) and 45 °C (T_2), respectively) in the heating process [30]. These aggregates showed extremely strong exciton coupling at wavelengths near the absorption of amide groups and pyridinium groups. The optical activity of amide groups changed from negative to positive around T_1 and optical activities of both groups disappeared above T_2 (Fig. 12a). Neither formation of tubular aggregates nor enhanced CD spectra were obtained from the corresponding ester-type compound at which dialkyl chains were introduced through ester bonds. These results indicate that the three amide bonds around the chiral carbon play an important role in

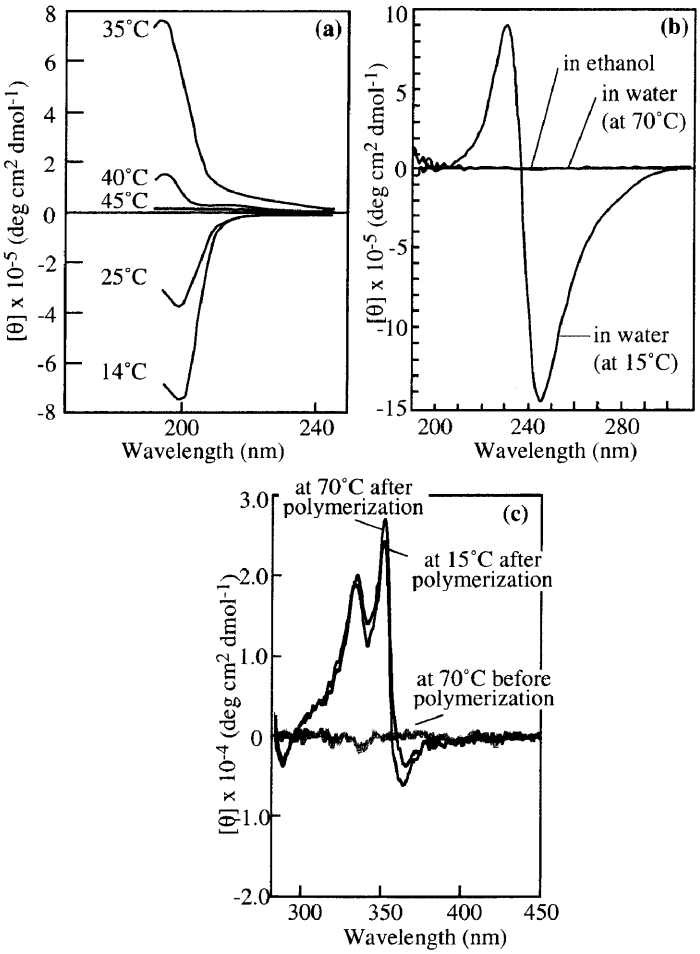

Figure 12. Specific optical activities in (a) **B-3** [30] and (b) **B-18** aggregates in aqueous solutions [32], and (c) **G-11** organogels [163]. (a) The optical activity changes reversibly depending on temperature. (b) The CD pattern indicates that the sorbyl groups as polymerizable moiety are in chirally stacking states among them at a temperature below T_c. (c) Polymerization of methylmethacrylate as a bulk solution promotes stabilization of the highly oriented structure of **G-11** aggregates [163]. Reprinted with permission from [30], H. Ihara et al., *J. Chem. Soc. Jpn.* 1047 (1990). © 1990, The Chemical Society of Japan; and from [32], H. Ihara et al., *Langmuir* 8, 1548 (1992). © 1992, American Chemical Society.

the formation of supramolecular assemblies. The reversal of chirality is probably due to change of the molecular orientation, for instance, from S-chiral to R-chiral. Similar induced CD spectra based on chirally ordered structure have been observed in bilayer aggeregates formed by chromophoric group-containing lipids (**B-11** and **B-18**).

Mirror-image of CD spectrum was obtained in bilayer membrane aggregates from D- and L-form lipids, respectively [84]. Specter et al. [116] reported on the CD spectra and TEM observations of diacetylenic phospholipid in various conditions. The CD spectra of R- and S-enantiomers showed similar patterns but opposite signs and the CD signal of racemic mixture showed approximately nothing. Moreover, TEM observations showed that the R- and S-enantiomers formed tubular aggregates with the same dimensions, and their racemates also formed tubular aggregates without dimensional changes. Since the tubular aggregates of pure enantiomers were grown from

left- and right-handed helical aggregates, respectively, it was anticipated that racemic mixture almost phase-separated.

It is well known that achiral dye molecules bound to chiral poly(α-amino acid) show CD spectra (induced circular dichroism (ICD)) around their absorption bands [117–119]. Similar phenomena have been observed on chiral bilayer assemblies. When an achiral dye molecule, such as methyl orange, was added to **B-4** aggregates in an aqueous solution, it combined with the cationic membranes to give three dispersion species, belonging to S-chirally oriented dimmers on the surface, monomers on the surface, and monomers incorporated into the bilayers, respectively [76]. Many chiral lipids possess similar functions through formation of highly oriented structures [85–87].

3.2.5. Stabilization of Fibrillar Assemblies

Compared with nano assemblies from lipids, carbon nanotubes are useful in light of their physical and chemical stability, but this stability causes limitations on modification. The assembling systems, however, provide unlimited opportunities for modification. For example, the mixing of L- and D-isomers of **B-1a** causes their racemates to show absolutely different morphologies from their original forms. **B-1b** ($n = 4$) can form only fragmented fibrillar aggregates spontaneously, but this morphology can be transformed to well-developed twisted ribbon-like aggregates by mixing with a triple chain-alkylated, lipid-forming tubular aggregates [32]. However, these morphological transformations mean to be so weak for their industrial use. Therefore, it must be valuable to stabilize their aggregates. This attempt has been carried out by physical and chemical methods. The chemical methods are roughly classified into three types as summarized in Figure 13. However, most of these methods include polymerization, and, thus, the resulting bilayer membranes lose some functions such as molecular fluidity instead of obtaining stability. Of course, stabilization is required in some cases to expand their applications.

Polymerizable lecithins (**B-15**) with diacetylenic alkyl chains such as 1,2-bis(10,12-tricosadi-ynoyl)-sn-glycero-3-phosphocholine ($DC_{8,9}PC$) are known to form tubular microstructures when their liposomes are cooled below the chain-melting transition [25]. Tubular and helical structures from **B-15** measured from 0.3 to 3 μm in diameter and from

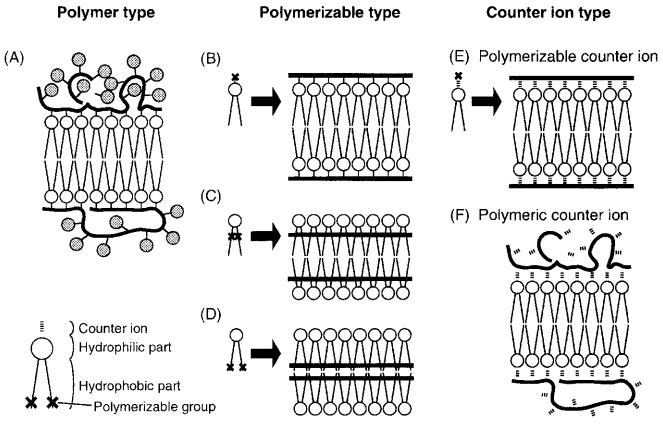

Figure 13. Stabilization of bilayer aggregates by polymerization.

5 to over 1000 μm in length. Both dimensions depended on the solvent system (ratio of water-to-alcohol). Irradiation with UV rays or γ-rays induced photopolymerization of diacetylenic units, but the helical or tubular structures were lost. A series of monoacryl and diacryl double-chain ammonium amphiphiles (**B-16** and **17**) were synthesized for investigation of their dispersion characteristics before and after photopolymerization [103]. **B-16** formed vesicular aggregates after dispersion into water and transformed into helices when allowed to stand at room temperature for 1 month. Polymerization of acryloyl groups leads to destruction of aggregation morphologies.

On the other hand, we reported the dispersion states and effect of polymerization on the aggregation morphology from polymerizable lipid (**B-18**) [32]. The introduction of polymerizable sorbyl groups at the end of the hydrophobic alkyl chains is far enough from the chiral carbon in order to prevent obstruction of the chiral interactions between lipids. **B-18** formed single-wall helical bilayer structures (Fig. 8u) with large chirality (Fig. 12b) in aqueous solutions below T_c (= 51 °C). Ultraviolet irradiation of the **B-18** aggregates caused photoreaction of the sorbyl groups at a rate 25 times faster in the stacked species (below T_c) than in the nonstacked species. This photoreaction was accompanied by morphological transitions from helical aggregates to tubular aggregates below T_c and to twisted fibrillar aggregates above T_c. Almost no morphological change was observed as a result of this polymerization over a wide range of temperatures.

3.3. Nanofibers in Organic Media

Hydrogels can often be formed from aqueous solutions of hydrophilic polymers, biomolecules such as proteins, and inorganic materials such as silicates. They have been studied in detail, and related books [120, 121] and reviews [122] have been published by many researchers. Some of these gels and gelators are widely used in industries, food science, and cosmetic science. Recently, it has been found that some specia, low molecular weight compounds formed gels in organic media [123]. These can be referred to as organogels (organic gels). Organogels are very unique, not only in that the gelation is induced by three-dimensional network formation with well-developed fibrous aggregates, but also in that these aggregates are on the basis of highly oriented structures like aqueous lipid bilayer membranes. Therefore, they attract our interest in spite of their instability, and we further label them "self-assembled organogels" to distinguish them from conventional gels. Self-assembled organogels include various fibrillar aggregates such as rods, helices, and sheets, and the challenge to stabilize their morphologies and molecular orientation to widen their applications is now being met. In this section, we focus on nanofibrillar aggregates formed in organic solvents.

Low molecular weight compounds that can produce gels from organic solvents have been known for 50 years. However, the gelation of organic solvents and oils as macroscopic phenomena has been a main subject of interest for several decades thereafter. From the late 1980's to the early 1990's, several kinds of organogels were discovered simultaneously. In this period, many researchers joined the research field

of nano-sized molecular architectures to develop molecular devices for supersensitive sensors, high-density memory storage, and so on. It appears that a point-of-view toward organogels has been shifted into explication and control of molecular buildings formed from low molecular weight organogelators, spontaneously. The original root compounds of organogelators (Fig. 14) have been discovered serendipitously by researchers who were working in various research fields [70, 124–127]. Therefore, the chemical structures of most organogelators are derived from intermediate molecules designed for specific functions.

3.3.1. On Driving Forces and Chemical Structures

A hydrophobic effect is the most essential driving force for molecular aggregates in aqueous solution systems but almost disappears in organic media. More positive intermolecular interactions play an important role in molecular aggregation in organic media. Hydrogen-bonding interaction is especially effective and many organogelators are classified into this category. 12-Hydroxystearic acid (12HSA, **G-6**) and its related salts were early examples of organogelators [128–130] and the first report of 12HSA was brought by Tachibana et al.

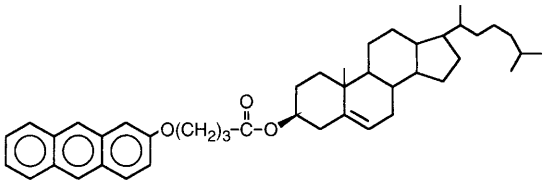

G-1 Cholesterol-based compound

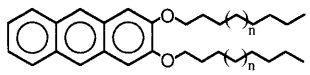

G-2 PAH-based compound

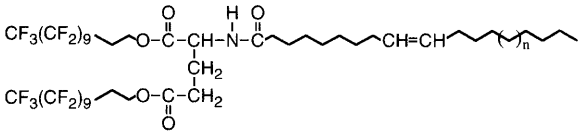

G-3 Perfluoroalkyl-based compound

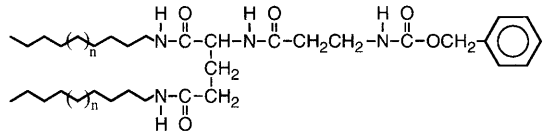

G-4 Peptide-based compound

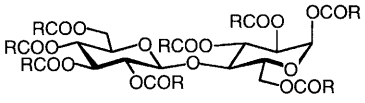

G-5 Saccharide-based compound

Figure 14. Root organogelators developed in the late 1980's to the early 1990's **G-1** [124], **G-2** [125], **G-3** [126], **G-4** [70], **G-5** [127].

in 1965. Lithium 12HSA forms twisted fibrous aggregates, whose direction of the twist depends on the optical isomerization of lithium 12HSA. Transmission electron microscopic observations show that the direction of the twist is left-handed for the L-form, but right-handed for the D-form, and that no twisted fibers are obtained for the DL-form. Furthermore, the helical structures formed from 12HSA are sensitive to counter metal ions. 12HSA forms developed ribbon-like aggregates with diameters of 10 to 100 nm in soybean oil. However, the number of cross-sections is relatively few according to SEM observations. Addition of sodium salt of 12HSA to these organogels contributes to improvement of gelation ability with metamorphoses from flexible ribbon-like aggregates to bundled rigid fibers with equal diameters. Terech et al. elucidated the oriented structure of 12HSA organogels at the molecular level by a combination of several techniques [131]. Small-angle neutron scattering (SANS), small-angle X-ray scattering (SAXS), and wide-angle X-ray scattering (WAXS) investigations revealed the structural model of the 12HSA fibrous or twisted, strand-like aggregates in organic media. The 12HSA molecules form head-to-head aggregates in fibrous networks and the growth of fibrous aggregate in the fiber axis direction is promoted by hydrogen bonds between the hydroxyl groups of 12HSA. A polarity of solvents influences the diameter of fibrous aggregates since the laminating of fibrous aggregates in the vertical direction is brought by dipole-dipole interactions between carbonyl groups of 12HSA. Microscopic morphological arrangements of fibrous aggregates inevitably lead to structural changes of cross-section and/or junction zones, and finally exterior transformations such as transparency (turbidity) and other physical properties will appear.

Peptide-based derivatives will be useful as organogelators because their amide bonds work as a stronger driving force for molecular aggregation. Peptide-based organogelators have a plural number of hydrogen bondable moieties. **G-4** [70, 73] as a typical example, possesses three amide bonds around an L-glutamic moiety, which works as a good organogelator. Transmission electron microscopic and SEM observations showed a three-dimensional network with fibrillar aggregates in its organogel and xerogel (Figs. 15a and 15b, respectively). The minimum diameter of the aggregates in the picture is 20 nm, which is 2–3 times larger than the molecular length estimated by SAXS [73]. However, if two of the three amide bonds are replaced by the ester bonds, no gelation is observed even when their concentration is 10 times higher than the former. It was also confirmed that addition of trifluoroacetic acid as an inhibitor for hydrogen bonding causes gel-to-sol transition. MOPAC calculation indicated that the three amide bonds around the L-glutamic acid moiety provided a proper conformation for intermolecular interaction.

K. Hanabusa et al. investigated the gelation abilities of single-chain alkylated mono- or dipeptides toward general organic solvents [132–134]. Peptides containing L-isoleucine and L-valine (**G-7**) work as distinguished gelators for various organic solvents such as alcohols, ketones, esters, dimethyl formamide (DMF), dimethyl sulfoxide (DMSO), and aromatic compounds. Both the length of the alkyl chain and the side chain structure of amino acids are important in the

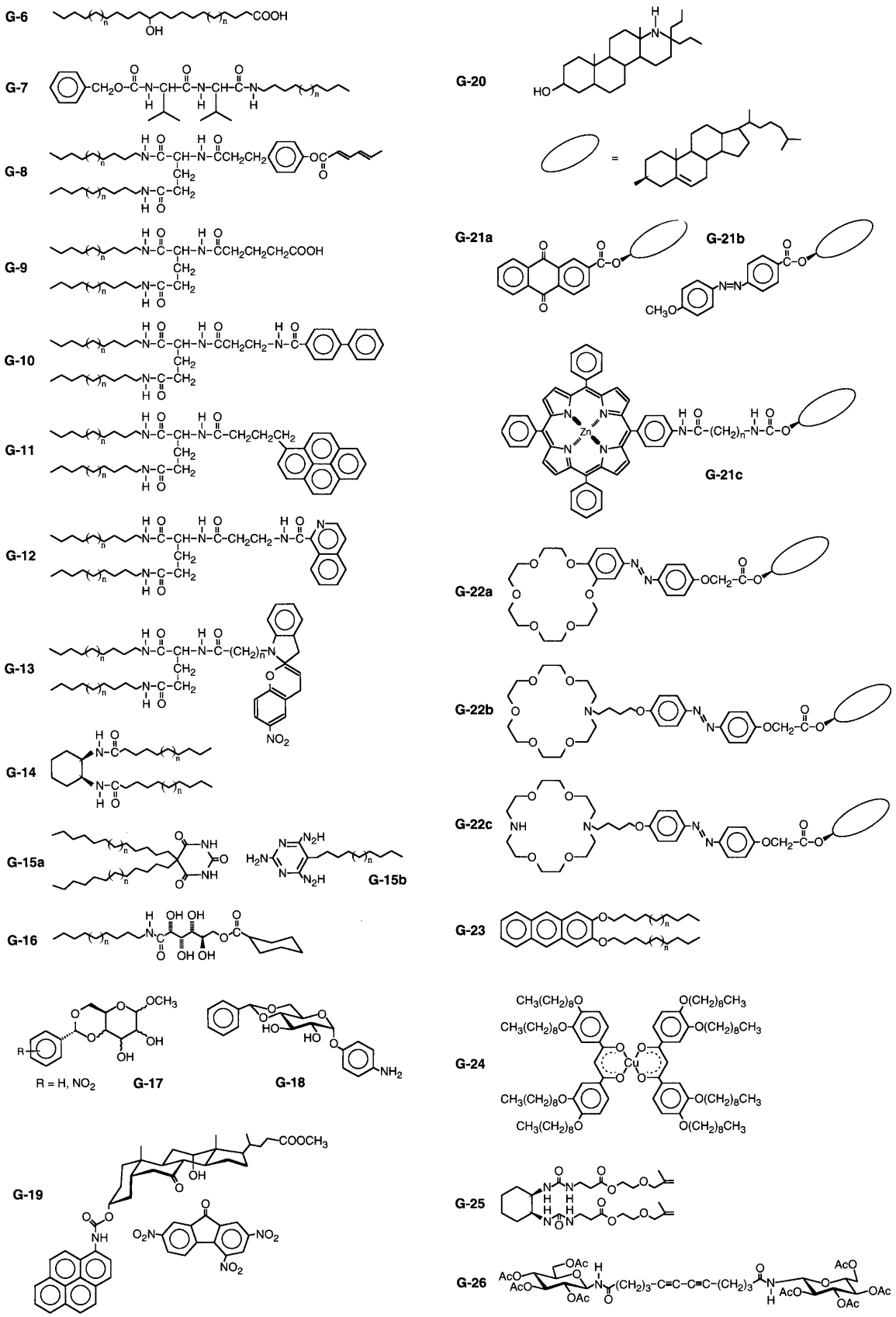

Figure 15. Chemical structures of various low-molecular mass organogelators (Ref.: **G-6** [128], **G-7** [134], **G-8** [157], **G-9** [169], **G-10** [213], **G-11** [80], **G-12** [172], **G-13** [83], **G-14** [135], **G-15a** [63], **G-15b** [63], **G-16** [138], **G-17**[215], **G-18** [78], **G-19** [147], **G-20** [123], **G-21a** [216], **G-21b** [176], **G-21c** [173], **G-22a** [177], **G-22b** [166], **G-22c** [166], **G-23** [214], **G-24** [151], **G-25** [158], **G-26** [159]).

production of fibrous aggregates. If a hexyl chain is introduced instead of an octadecyl chain, the compound neither produces organogels in solvent nor forms fibrous aggregates. The possible structure for the long chain-alkylated dipeptides was proposed to be an antiparallel β-sheet through intermolecular hydrogen bonds between the amide and urethane groups.

Cyclohexane diamide derivatives have hydrogen bonding sources [135, 136]. Although the two isomers of *trans*-1,2-cyclohexane diamide derivatives (**G-14**), which are (1R, 2R) and (1S, 2S), can produce a gel for many organic solvents, *cis*-isomer derivatives have no gelation ability. Furthermore, dialkylated 1,3- and 1,4-cyclohexane diamide derivatives did not produce organogel. It was considered from their aggregation morphologies that one-dimensional growth of molecular assemblies through intermolecular interactions was indispensable to the formation of fibrous aggregates. The alkyl chains connected to the *cis*-isomer are spread spatially since they are located at axial and equatrial positions, respectively. The molecular packing formation in the aggregates is also important for one-dimensional growth and this can also apply to 1,3-isomers and 1,4-isomers.

A two-component gelation system revealed essential information about the gelation mechanism. A pair of compounds, **G-15a** and **G-15b**, was designed as a two-component system because a dumbbell-type cocrystal was produced from a barbiturate derivative and triaminopirimidine through the intermolecular hydrogen bonds [63]. The heating process normally carried out to dissolve an organogelator into the solvents is unnecessary to produce organogels in chloroform with the combination system of **G-15a** and **G-15b**. Molecular orientation of the two-component system was supported by FT-IR and SAXS measurements. Transmission electron microscopic observations show the twisted fibrous aggregates in organic solvents. Since each molecule cannot form an organogel individually, it is understandable that the arrangement of the hydrogen bond-forming moiety and bulkiness of the molecule are important in inducing self-assembled organogels. This argument is supported by the results of dendritic two-component gels. Dendrimetric peptides with carboxylic acid form organogels with a linear aliphatic diamine in nonhydrogen bonding solvents [137].

Saccharide-based lipophilic derivatives (**G-5** and **G-16**) can be organogelators. Hafkamp et al. reported that gluconamide derivatives (**G-16**) form stable organogels in a number of solvents such as *o*-xylene, chloroform, and ethyl acetate [138]. Transmission electron microscopic observations showed that **G-16** formed fibers or bundled fibers. Studies of gluconamide derivatives were carried out to explicate gelation mechanisms. **G-16**, whose free hydroxyl groups were protected by bismethylene, was synthesized to confirm the effects of free hydroxy groups on the formation of organogels. Since these compounds did not form organogels in any solvents, it was clarified that the hydroxyl groups played an important role in the gelation.

Since saccharides have many hydrogen-bonding sources, they are, like amino acids, invaluable materials for design of organogelator molecules. Friggeri and Gronwald et al. have reported 11 methyl 4,6-benzylidene derivatives of the monosaccharides D-glucose, D-mannose, D-allose, D-altrose, D-galactose, and a-D-isose (**G-18**) [139–141]. The driving force of aggregation was estimated as intermolecular hydrogen bondings by FT-IR and ^{1}H-NMR spectroscopies. Gelation ability was evaluated in a large number of organic solvents, and it was found that insignificant differences among the chemical structures are effective decisively on their gelation ability. Furthermore, a remarkable change in molecular mobility around T_{gel} was observed by the line-broadening effect of ^{1}H-NMR. Structural details in fiber network in the solid state and gel state were deduced by ^{1}H-NMR, FT-IR, and SAXS. The series of these sugar-based derivatives is useful to construct architectures of molecular assemblies as base compounds.

There are some derivatives that can produce organogels without intermolecular hydrogen-bonding interaction. A typical example is the steroid derivative with polyaromatic group (**G-1**), first reported in 1987 by Weiss et al., who investigated the gelation ability of the isoandrosterone derivatives [124, 142–144]. The kinetics were investigated in detail by using electron paramagnetic resonance (EPR), SANS, infrared (IR), and CD spectroscopies. After this finding, more than 40 derivatives, including steroid and aromatic groups, have been reported. They are sometimes classified by the abbreviations ALS, where A, L, and S correspond to aromatic (A), linking (L), and steroid (S) groups, respectively. Effects of chemical structures of each part on the gelation were investigated in detail; for instance

1. stereo-chemistry at C-3 and the nature of the chain at C-17 of the steroidal part,
2. various aromatic groups such as 9,10-anthraquinones, cinnamate, 2-naphtyl, 1-pyrenyl, phenyl, and their substituted compounds,
3. the length and functionality of the linking groups.

Several important considerations for organogelators from aromatic compound-linked steroid were concluded as follows [145]:

1. H-bonding, even when possible, may be absent in low molecular-mass organic gelator (LMOG) assemblies when other packing contributions (e.g., π-π interaction and London dispersion forces) dominate [146].
2. Charge-transfer interactions within gelator strands can stabilize gels [147].
3. Thixotropy can be induced by adding a small concentration of a second (nongelling) ALS molecule whose size and shape are similar to those of a good ALS gelator.
4. The fraction of ALS gelator within the solid network is dependant on temperature and on the solubility of the gelator in the liquid component [143, 144].
5. The bulk properties of a liquid mixture, rather than the properties of the individual components, determine the dimensions and shape of the gelator assemblies [142], as well as the relative ordering of T_{gel} values within a series of ALS gelators.
6. Subtle changes in molecular shape can alter profoundly the ability of an ALS to gel organic liquids.

Inductions of functional groups such as crown ether and azo-benzene into cholesterol were performed by Shinkai et al. [175–177]. Application of these organogelators are described in Section 3.3.4.

We estimate that a steroid group will give limited solubility to organic solvents compared to a long chain alkyl group and thus may work as a sorbophobic moiety. Positive interaction can probably be induced by polyaromatic groups. Supporting this, anthryl derivatives connected to dialkyl chains have been studied as organogelators [125, 148–150] 2,3-Bis-*n*-decyloxyanthracene, **G-23**, produced organogels in many organic solvents [125]. Since 2,3-dialkoxynaphthalene showed no ability of gelation for any organic solvents, increasing aromaticity promoted gelation ability. Even if the anthracene moiety was replaced by anthrax quinone and phenazine, effective gelation was observed. The number and length of alkyl chains were also sensitive to gelation abilities. Freeze-fracture electron micrographs of **G-23**-propanol gels indicated a three-dimensional network of fibrous rigid bundles with 60–70 nm diameters.

Some organometallic compounds can also be organogelators, in which case the essential interaction source is surely derived from the chelation behavior. Terech et al. reported that mononuclear copper β-diketonate derivatives **G-24** formed both organogels [151] and thermotropic disc-like mesophases in cyclohexane [152, 153]. Some binuclear copper tetracarboxylates [154–156] form neat thermotropic columnar mesophases and organogels at less than 1 wt% concentrations in hydrocarbons. These organogels form disc-like molecules including semi-rigid, rod-like threads whose diameter was 1.7 nm, which corresponds to the diameter of disc-like molecules.

At the end of this section, chemical structures and aggregation forms of low-molecular organogelators are summarized in Fig. 16 and Table 1.

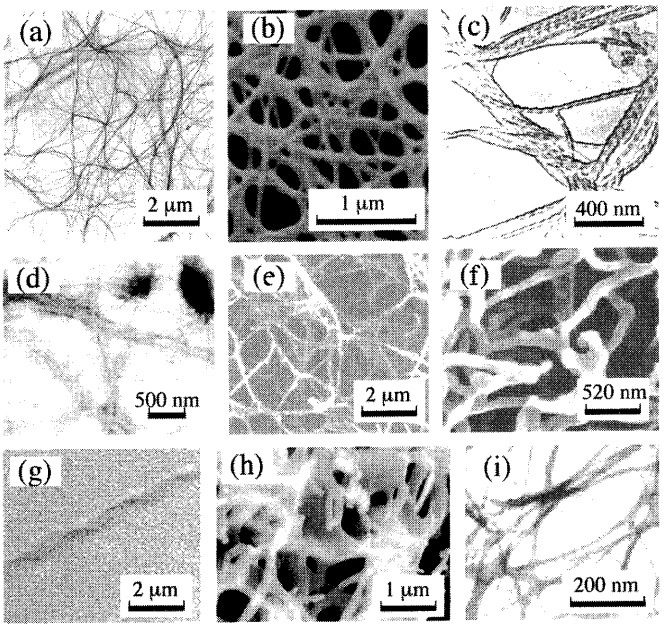

Figure 16. Fibrillar networks formed from various low-molecular mass organogelators (a) **G-4** [70], (b) **G-4** [73], (c) **G-20** [123], (d) **G-7** [134], (e) **G-25** [158], (f) **G-17** [215], (g) **G-5** [127], (h) **G-21c** [173], (i) **G-26** [159]. Reprinted with permission from [123], P. Terech and R. Weiss, *Chem. Rev.* 97, 3133 (1997). © 1997, American Chemical Society; from [134], K. Hanabusa et al., *J. Chem. Soc. Chem. Commun.* 390 (1993). © 1993, Royal Society of Chemistry; from [158], M. de Loos et al., *J. Am. Chem. Soc.* 119, 12675 (1997). © 1997, American Chemical Society; from [215], K. Yoza et al., *J. Chem. Soc., Chem. Commun.* 907 (1998). © 1998, Royal Society of Chemistry; from [173], T. Ishi-i et al., *J. Mater. Chem.* 10, 2238 (2000). © 2000, Royal Society of Chemistry; and from [159], M. Masuda et al., *Macromolecules* 31, 9403 (1998). © 1998, American Chemical Society.

3.3.2. Chemical Stabilization of Organogels

Some lipophilic peptides have been investigated not only as organogelators but also with respect to their self-assembling behaviors. This latter property gives them distinct advantages compared with conventional gel systems. The fibrillar aggregates are based on highly ordered structures, and thus show aqueous lipid membrane-like behaviors such as phase transition, phase separation, and chirality enhancement through molecular orientation. Although these features are advantageous for extended applications, it is also clear that their thermal and mechanical instabilities are a disadvantage in some application fields.

Some approaches have been proposed for stabilization of organogels. Introducing polymerizable group into a gelator is a reasonable method for this purpose. The first example of polymerizable organogelator was a sorbyl group-introduced peptide (**G-8**) in 1995. In this case, significant stabilization was not observed by photo-induced cross-linking among the peptides because oligomerization was a predominant reaction in the process [157]. On the other hand, de Loos et al. reported a bis(ureido)cyclohexane derivative containing a methacrylate moiety as a polymerizable organogelator (**G-25**) [158]. This compound produces organogels with developed fibrous aggregates in various organic solvents. Gel formation was maintained after polymerization by UV irradiation in the presence of a photo-initiator and the resultant gel showed highly thermal stability up to temperatures above the boiling point of the solvents. Polymerization of photo-induced polymerizable groups containing organogelators (**G-26**) was demonstrated by Masuda et al [159, 160]. Diacetylene containing organogelator (bolaamphiphile) was used for the purpose of stabilizing. Polymerization could be monitored by UV spectroscopic observations, and was induced by photo or γ-ray irradiation. In each case, stability of the organogel preserving fibrous aggregates rose in several samples after polymerization. However, reversibility of sol-to-gel transition and most properties based on molecular fluidity disappeared.

Sometimes, metal ions increase the mechanical strength of organogels. 1-O-(*p*-Aminophenyl)-4,6-O-benzylidene-α-D-glucopyranoside (**G-18**) behaves as a good gelator for various organic solvents [78, 139]. The T_{gel} values for ethanol gel were markedly improved by addition of $AgNO_3$, $CoCl_2$, or $CdCl_2$. The T_{gel}s for 1 wt/vol% of organogel in ethanol are -10 °C and 71 °C, respectively, in the absence and presence of equimolar $CoCl_2$. This remarkable change is due to cross-linking of **G-18** molecules by Co(II)-amino group interaction. It seems that hydrogen bonds and coordination bonds work cooperatively for reinforcement of organogels. Similar observations were obtained using a diketonate ligand-containing organogelator [161]. Maitra et al. reported that the donor-acceptor interaction promoted

Table 1. Classification of self-assembling organogelators.

			Structual unit											Driving force for aggregation	Aggregates		Notes
			Nonpolar moiety					Polar moiety									
Ref.	Compound	Year	sac	dac	mac	cho	pah	Acidic	Basic	Saccha-ride	Peptide	Amide urea			Diameter (nm)	Form	
[128]	L, D	1965	*					*						hb	10–100	tr	**G-6**, Figure 15
[63]	1 + 4	1993	*	*					*					hb	80	msf	**G-15a** + **G-15b**, Figure 15
[134]	6	1993	*								*			hb	100–300	tr	**G-7**, Figures 15 and 16d
[217]	6	1994	*				*							hb, sp	8–10	ssf, msf	**G-3**, perfluoroalkyl-containing, Figure 14
[138]	4	1997	*							*				hb, mc	ca. 40	hr	**G-16**, Figure 17a
[159]	1	1998	*							*				hb	3–20	ssf, msf	**G-26**, polymerizable, Figure 15 and 16i
[218]	3	1999	*				*							hb	15–40	hr	bolaamphiphiles
[219]	1	1999	*								*			hb	—	ssf	
[220]	1	2000	*									*		hb	30–100	msf	
[221]	1	2000	*				*							sp, pp	6–25	ssf, msf	stilbene-containing
[222]	2	2001	*								*			hb	30–100	msf	
[223]	1	2001	*					*			*			hb	0.5–15μm	ssf	
[224]	9b	2002	*											hb, sp	10–12	ssf	cholate-containing
[225]	6	2002	*				*	*				*		hb, pp	50–70	ssf	
[125]	DDOA	1991		*			*							pp	60–70	msf	**G-2**, anthracene-containing, Figure 14
[70]	2	1992		*			*				*			hb	—	—	azobenzene-containing
[226]	5a	1995		*							*			hb	3	ssf, msf	**G-8**, polymerizable, Figure 15
[136]	4, 5	1996		*								*		hb, pp	20–80	msf	
[135]	1, 2	1996		*								*		hb	40–70	tr	**G-14**, Figure 15
[83]	2	1997		*			*				*			hb	—	ssf, msf	**G-13**, piran-containing, Figure 15
[227]	2	1997		*								*		hb	50	msf	**G-25**, polymerizable, Figures 15 and 16e
[213]	2	1999		*			*				*			hb, pp	—	—	**G-10**, biphenyl-containing, Figure 15
[228]	D-1	1999		*				*			*			hb	—	hr	**G-9**, Figure 15
[229]	1a	1999		*							*			hb	40–100	ssf, msf	**G-4**, Figure 14 and 16a
[230]	1	1999		*			*					*		hb, pp	2–10	tr	
[231]	1	2000		*					*		*	*		hb	20	ssf, msf	
[232]	2	2000		*			*					*		hb	20–70	ssf	porphyrin-containing
[214]	1	2000		*			*							pp	—	ssf	**G-23**, anthracene-containing, Figure 15
[233]	2	2001		*			*				*			se, hb	30	ssf, msf	bipyridinium-containing
[234]	2	2001		*								*		hb	—	msf	
[235]	2	2001		*			*					*		hb, pp	—	—	azobenzene-containing
[236]	3	2002		*								*		hb	—	ssf, msf	polymerizable
[237]	1, 2	2002		*			*					*		hb, pp	10–20	ssf	azobenzene-containing
[80]	2	2002		*			*				*			hb, pp	—	ssf	**G-11**, pyrene-containing, Figure 15

[172]	1	2002	*				*		*		hb	50–100	msf	**G-12**, Figure 15
[151]		1987		*							sp, mc	—	—	**G-24**, Figure 15
[238]	1a	1995		*		*					pp	6	ssf, msf	crown ether- and phthalocyanine-containing
[127]	CB 10	1995		*				*			sp	—	—	**G-5**, Figures 14 and 16g
[162]	TOAB	1997		*			*				sp	240–1400	ssf, msf	
[239]	2	2000		*							pp, mc	3.5–3.4	tu	olefine- and crown ether-containing
[80]	1	2002		*		*			*		hb, pp	—	ssf	porphyrin-containing
[240]	2	2002		*						*	sp	50–250	tu	perfluoroalkyl-containing
[241]	CAB	1987			*	*					sp, pp	16–19.2	msf	**G-1**, Figure 14
[175]	1, 2, 3	1991			*	*					pp	100	msf	**G-22**, azobenzene- and crown ether-containing, Figures 15 and 18
[176]	3R′	1994			*	*	*				sp, pp	—	hr	**G-21b**, azobenzene-containing, Figure 15
[177]	13Me	1998			*	*	*				sp	—	ssf	azobenzene-containing
[242]	S, R	1998			*	*					sp, pp	10–50	ssf	porphirin-containing
[147]	4 + 6	1999			*	*					sp, ct	2 mm	ssf	**G-19**, pyrene-containing, Figure 15
[243]	1	2002			*	*					se, pp	500	tu, hr	crown ether-containing
[244]	PFS-b-PDMS	1998				*					ct	20	tu	ferrocene-containing, polymer
[245]	4b	2001				*					pp	100–150	—	
[246]	PBZT	2002				*					pp	10	—	
[247]	Ib	1999						*			hb	20–120	msf	**G-18**, Figure 15
[248]	Z-1	1999							*		hb	—	tu	azobenzene-containing
[249]	9	2000							*		hb	20–50	—	cyclic dipeptide
[250]	1	2001							*	*	hb	20–50	tu	
[251]	P_{11}	2001							*		hb	—	tr	origopeptide
[252]	6	1997								*	hb	—	—	
[253]	1 + 3	1999								*	hb	20–50	—	
[254]	1	2000								*	hb	30–300	msf	
[255]	3, 4	2000								*	hb	20	msf	
[256]	4b	2001								*	hb	50	—	cholate-containing
[257]	1	2001								*	hb	15	msf	
[123]	STNH	1997									sp	ca. 40	tr	**G-20**, Figures 15 and 16c
[215]	1	1998									sp	30	ssf	**G-17**, Figures 15 and 16f

Note: sac: single-chain alkyl, dac: double-chain alkyl, mac: multiple-chain alkyl, cho:cholesterol-containing, pah: polycyclic aromatic hydrocarbons, ssf: single-strand fiber, msf: multi strand fiber, tr: twisted ribbon, hr: helical ribbon, tu: tubles, hb: hydrogen bonding, sp: solvophobic effect, mc: metal-coordinate interaction, pp: π-π interaction, ct: charge transfer interaction.

organogels (**G-19**) [147]. Pyrene-containing bile acid derivatives formed highly stable organogels with needle-like aggregates in various solvents even with less than 1% of the gelator. The T_{gel} increased with increasing amounts of trinitrofluorenone as an electron acceptor that could not form a gel in solvents. In an organogel system, several intermolecular interactions participate to maintain the gel formation. Control of these interactions is useful not only for understanding the gelation mechanism but also for developing functional organogels.

3.3.3. Approach for Nanostructured Materials

Organogel systems can be applied as a liquid organic media. Gu et al. [162] and Hafkamp et al. [138] described morphological imprinting of fibrous aggregates using tetraoctadecylammonium bromide and gluconamide derivatives coordinated with metal ion, respectively. Each organogelator can produce organogels with fibrous aggregates in styrene and methyl methacrylate. Polymerization of the solvents was carried out with UV light in the presence of a photoinitiator. Fibrous aggregates with similar diameter were observed before and after photo-polymerization, and the gelator molecules could be removed from the resultant polymer matrix by the solvent extraction method (Fig. 17) [138]. According to optical and electron microscopic measurements, the diameters of the strand-like pores were bigger than those of the original fibrous aggregates. It was expected that the monomers that exist near the surface of fibrous aggregates could not react since their mobility and fluidity were restricted. Similar observations were obtained with organogels from a pyrenyl group-containing peptide lipid (**G-11**) in styrene and methylmethacrylate. In this study, we obtained significant information on the molecular orientation states before and after polymerization of the bulk solution. Enhanced CD spectra around the pyrenyl group was observed after polymerization and maintained even at 70 °C, a temperature was even higher than its T_{gel}. These results indicate that highly oriented structures can be stabilized by polymerization of a bulk solution [163].

Ono et al. have reported that hollow, fibered silicas are prepared by transcription of various suprastructures formed in organogels [164, 165]. Three cholesterol-based gelators with monobenzo-18-crown-6 (**G-22a**), monoaza-18-crown-6 (**G-22b**), and 1,10-diaza-18-crown-6 (**G-22c**), respectively, were synthesized. These compounds produced organogels. Scanning electron microscopic observations of the xerogels showed that their organogelators assemble into a fibrous network structure, a curved lamellar structure, and a cylindrical tubular structure, respectively, in cyclohexane. Sol–gel polymerization of tetraethoxysilane was carried out in each of the gel systems. The silica obtained from **G-22a** showed a granular structure and a hollow fiber structure featuring the rough surface and the thick tube wall, respectively, in the absence and the presence of metal. This structure was created by adsorption of the anion-charged silica particles onto the cation-charged organogel fibers. On the other hand, the silica obtained from **G-22b** and **G-22c** had a hollow fiber structure featuring a smooth surface and thin tube wall both in the absence and the presence of metal salt. In the absence of metal salt, it was considered that the cationic charge generated by protonation of azacrown ethers plays a crucial role in the creation of such hollow fiber structures. In the presence of $KClO_4$, sol–gel polymerization resulted in tubular silica with a multilayered structure like a roll of paper (Fig. 18) [166]. The findings suggested that sol–gel polymerization proceeded along the surface of the curved lamellar stucture of **G-22b** or **G-22c** and the silica eventually grew

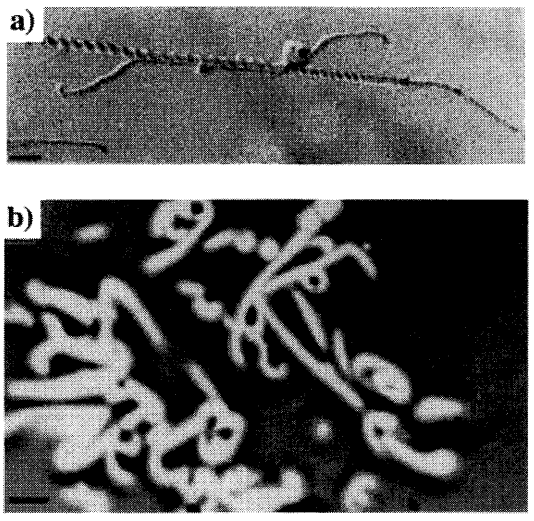

Figure 17. TEM images (Pt shadowing, bar 110 nm) of a dried gel (a) of **G-16** [138] in ethyl acetate and imprinted pores (b) of **G-16** [138] (bar 1.35 μm). Reprinted with permission from [138], R. J. H. Hafkamp et al., *Chem. Commun.* 545 (1997). © 1997, Royal Society of Chemistry.

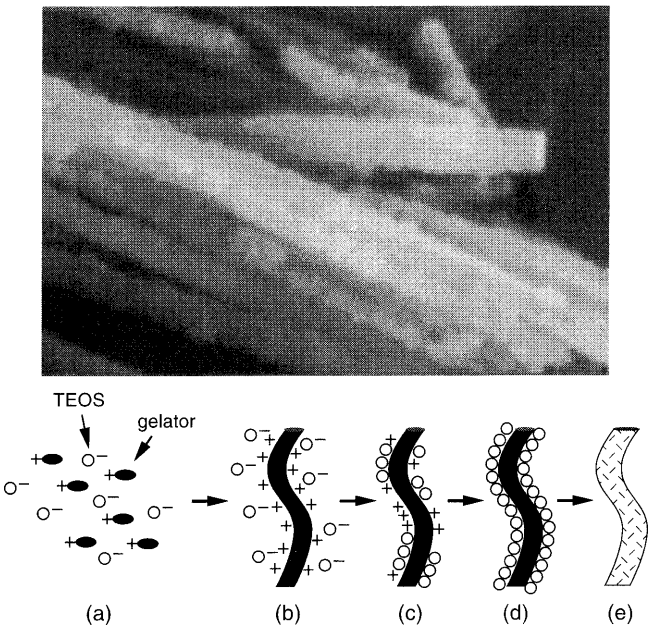

Figure 18. Schematic representation for the creation of hollow fiber silica by sol–gel polymerization of TEOS in the organogel state of **G-22** [166]: (a) mixture of gelators and TEOS; (b) gelation; (c) sol–gel polymerization of TEOS and adsorption onto the cationic gelator fibrils; (d) before calcination; (e) the hollowfiber silica formation after calcination. Reprinted with permission from [166], J. H. Jung et al., *Langmuir* 16, 1643 (2000). © 2002, American Chemical Society.

into a tubular structure. Vesicular and helical silica structures with several tens to several hundreds nm in diameter were obtained by using similar methods [166–168]. Future studies will certainly realize the production of more complicated and uniform nano-transcribed materials with desired fashion.

3.3.4. Control of Highly Ordered States

Some organogelators form highly ordered structures like those in aqueous bilayer membranes. Therefore, it is a convenient method to arrange the functional groups in the molecular assemblies. The arrangement and control of functional groups will certainly be an invaluable technique in many application fields such as sensors, molecular devices, and nano fabrication.

Lipophilic peptide-derived organogelators such as **G-10** and **G-11** show specific chirality, which is detectable by CD spectroscopic measurement around the chromophore groups. We have made some examinations to confirm whether or not specific properties observed in aqueous bilayer membranes can be reproduced in organic solvents. Phase separation behavior was observed in a mixture of **G-4** and an azobenzene-attached **B-4** derivative in benzene. Distinct CD spectra based on the azobenzene moiety were observed below T_{gel} [69]. The cotton effect of this mixture disappeared above T_{gel} and thermal reversibility was observed. On the other hand, a carboxylic acid-containing L-glutamate derivative (**G-9**) produced organogel with developed fibrous aggregates in several organic solvents [169].

These specific chiral properties stimulated us to implement optical resolution with chiral organogels. We reported the first example in 1995. When danoyl phenylalanine as a chiral guest molecule was dissolved in organogels from **G-4** and **B-3**, distinct enantioselective elution to an alkaline solution was observed. Interestingly, CD and DSC measurements showed that the best result was obtained through **B-3** domain formation phase separated from G-4 aggregates [170].

This finding encouraged us to control the chirality of organogels. For this purpose, we synthesized a double-chain alkyl L-glutamide derivative with an isoquinoline-head group (**G-12**) [171, 172]. This behaves as an organogelator with developed twisted fibers. It was confirmed that chelation with metal chloride in cyclohexane-ethanol (100:1) solution remarkably perturbed the chirality and morphology of the aggregates. Addition of copper ion ($CuCl_2$), which can form a square planar coordination, induced the chirality enhancement with morphological change from twisted fibrous aggregates to ribbon-like aggregates. On the contrary, cobalt ion ($CoCl_2$) and zinc ion ($ZnCl_2$), which can form an octahedral coordination state, caused serious morphological change with remarkable decrease of the chirality [171, 172].

On the other hand, Ishi-i et al. reported that a Zn(II)-porphyrin appended-cholesterol organogelator (**G-21c**) interacts with [60]fullerene to form a 2:1 Zn(II) porphyrin/[60]fullerene sandwich complex [173, 174]. The distinct bathochromic shift of the soret absorption band, which was found in the organogel with [60]fullerene in toluene, indicates that intermolecular electronic interaction exists between the Zn(II) porphyrin moiety and the [60]fullerene in the gel phase. Circular dichroism measurements suggested that the Zn(II) porphyrin moieties are strengthened to orient chirally in the gel phase by the interaction with [60]fullerene. The formation of a Zn(II) porphyrin/[60]fullerene sandwich complex would induce a morphological change-in-pitch length of twisted fibrous aggregates.

Light and metal ion-responsive organogelators were demonstrated by Murata and Shinkai et al. [175–177]. These gelators appended a crown ether moiety (**G-22a**), azacrown ether moiety (**G-22b** and **22c**), and azobenzenyl moiety (**G-21b** and **G-22**) to cholesterol, respectively. The azobenzenyl appended-cholesterol derivatives with a natural (S)-configuration at C-3 and those with an inverted (R)-configuration at C-3 formed organogels, but their solubilities and gelation abilities toward each solvent were quite different. LD, CD, and UV spectroscopic measurements showed that the azobenzene moiety was oriented in clockwise (in (R) chirality) or anticlockwise (in (S) chirality) direction when they interacted in the excited state. Furthermore, a sol–gel phase transition was induced by photoresponsive *cis*-trans isomerism of the azobenzene moiety. The molecular arrangement of crown ether appended-cholesterol derivatives was altered by the addition of metal ions and ammonium ion. The T_{gel} of this organogelator in methylcyclohexane/benzene (4:1) increased with increasing concentration of Li^+, Na^+, K^+, Rb^+, and NH_4^+, but decreased with increasing concentration of Cs^+. It was presumed that the 1:2 metal/crown complex with Cs^+ resulted in a disordered structure of organogels, but contrarily that 1:2 metal/crown complex with other metal ion and ammonium ion promoted their stability.

3.4. Nanofibrillar Structures from Polymers

3.4.1. Phase Separation Method

It is well known that block copolymers consisting of two or more compositions will form cube-like, rod-like, vesicle-like, and even lamella-like shaped microphase separation structures depending on the membrane casting conditions [178–185]. Therefore, it is also possible to produce a nanofibrillous microphase separation structure by choosing the chemical composition and varying the membrane casting conditions [186–193].

Liu et al. and Yang et al., for example, succeeded in producing a nanofibrillar-like microphase separation structure from A-B-C block polymers resulting from the combination of polystyrene (A), poly(2-cinnamoylethyl methacrylate) (B), and poly(tert-butyl acrylate) (C) (**P-4**) (Fig. 19a) [190]. To briefly introduce the method of production, a toluene solution of polymer was put into a polyethylene capsule, and a solid was obtained by evaporation and annealing. Transmission electron microscopic observation of the section of this solid showed a very beautiful nanofibrillar-like microphase separation structure with a diameter of about 25 nm as seen in Figure 19b [192].

On the other hand, Fujiwara and Kimura succeeded in producing a nanofiber from A-B or A-B-A block copolymer by the cast method from solution [191]. Specifically, it was obtained from a 0.2 wt% solution of block copolymer from poly(L-lactide) (A) and poly(oxyethylene) (B) which

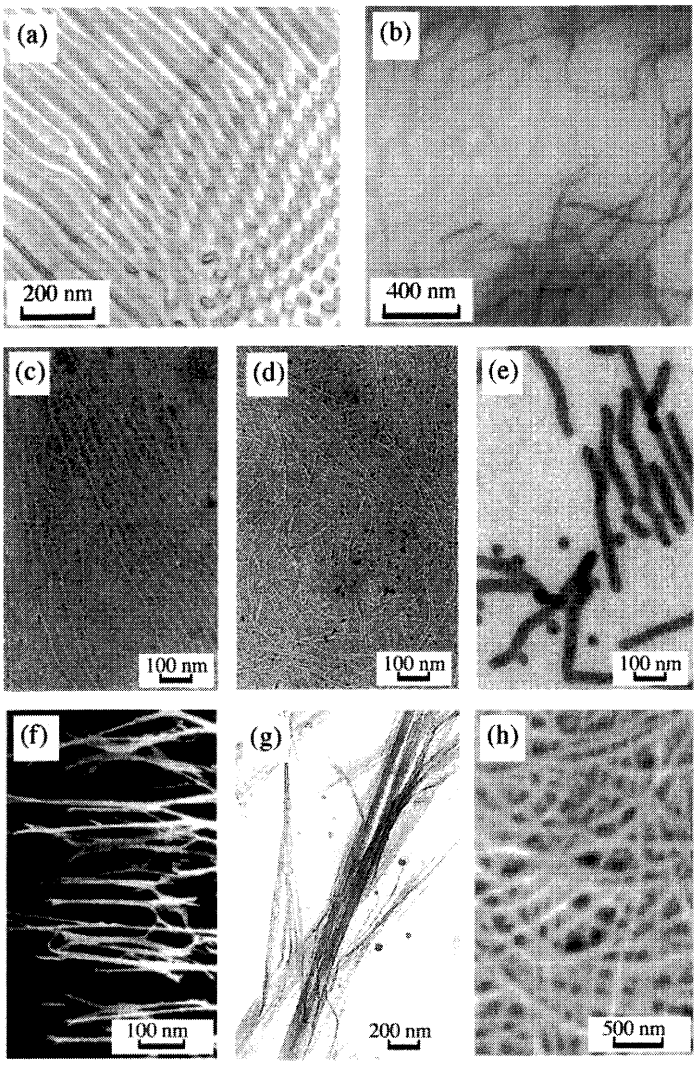

Figure 19. TEM images of (a) a 50-nm-thick section of a PS-b-PCEMA-b-PtBA/hPS film and (b) triblock/Fe_2O_3 hybrid nanofibers [192]. TEM images of the copolymer samples exfoliated from a silicon wafer surface after annealing at 60 °C for 10 h: (c) PLLA-PEG [191], (d) PLLA-PEG-PLLA [191], and (e) P4VP-(20.7)-b-PS(21.4k) diblock copolymers [187]. SEM images of (f) the self-synthesized PAN nanofibers [199], (g) the PPP nanofibers [198], and (h) electrospun fibers of polystyrene [197]. Reprinted with permission from [192], X. Yang et al., *Angew. Chem. Int. Ed.* 40, 3593 (2001). © 2001, Wiley-VCH; from [191], T. Fujiwara and Y. Kimura, *Macromol. Biosci.* 2, 11 (2002). © 2002, Wiley-VCH; from [187], K. de Moel et al., *Chem. Mater.* 13, 4580 (2001). © 2001, American Chemical Society; from [199], L. Feng et al., *Angew. Chem. Int. Ed.* 41, 1221 (2002). © 2002, Wiley-VCH; from [198], B. Yu and H. Li, *Mater. Science Eng.* A325, 215 (2001); © 2001, Elsevier; and from [197], A. G. MacDiarmid et al., *Synthetic Metals* 119, 27 (2001). © 2001, Elsevier Science.

was prepared (**P-5**), cast on mica, and afterwards annealed for 2 hs at 60 °C. From TEM observation, the diameter of the nanofiber formed from the A-B block copolymer was about 20 nm (Fig. 19c) [191], and that from the A-B-A block copolymer was about 6 nm (Fig. 19d) [191]. The authors hypothesize that the core is made from lactide (A) and that this part has a crystal structure.

de Moel et al. have proposed the crew-cut method as a new technique of attaining nanofibrillar microphase separation structures from block polymers like polystyrene (A) and poly(4-vinylpyridine) (B) (**P-6**) which are difficult to separate [187]. Specifically, a 1:1 complex was produced by adding equimolar amounts of pyradine and 3-pentadecylphenol (PDP) to a chloroform solution of A-B block polymer. This was then evaporated very slowly by drying at 50 °C for at least 12 hs. Next, a 0.5 g sample was put into a dialysis tube filled with ethanol, and most of the PDP(s) were removed by dialyzing for 2 weeks. Decompression dryness was carried out at 50 °C after washing by ethanol overnight, and a sample was obtained. Transmission electron microscopic observation showed that a nanofiber with a diameter of about 30 nm was formed from (A) in the core part (Fig. 19e) [187].

3.4.2. Injection Molding Method

When using a high polymer, it is possible to produce nanofibers by adapting an injection molding method. Although production of the nanofiber from a high polymer is somewhat forced, two techniques may be used: either injecting high polymer solution into nanosize pores [194–197] or polymerization and pushing out from nanofiber-like capillaries [198].

Feng et al. reported the production of nanofibers using the former technique by injecting poly(acrylonitrile) as a template into porous anodic aluminum oxide (Fig. 19f) [199]. Yu and Li adapted the latter technique with porous metal using poly(*p*-phenylene) (**P-7**) as a template to produce nanofibers (Fig. 19g) [198]. Features such as super-hydrophobicity [200–203] and erection luminescence [204–206] were obtained using both injection methods, but the nanofibers produced also had disadvantages such as low diameter uniformity and a tendency to become condensed.

In order to solve these problems, a technique called the electrospinning method has come into practical use. This technique was patented in 1934 by Formhals [207] and was little known at first, but it has been attracting attention for the past several decades as a nanomanipulation technique [208–211]. The electrospinning method is the technique of putting polymer solution and metal electrodes into a poor solvent such as water, and blowing off the polymer solution by applying high voltage between it and the metal electrodes, and producing nanofibers. In this case, the diameter and length of fibers formed depends on the concentration of polymer solution, the distance between the polymer solution and metal electrodes, and the voltage applied. MacDiarmid et al. have reported nanofibers formed using this technique with an average diameter of about 50 nm, by injection using a 2 wt% poly(aniline) chloroform solution and applying a voltage of 25,000 V from a distance of 25 cm [197]. Polystyrene nanofibers of about 30 nm in diameter were also prepared using the same technique, meaning that micron-order fibers can be prepared from nanofibers cheaply and easily (Fig. 19h).

4. SUMMARY

"Self-assembled nanofibers" are formed from miscellaneous synthetic compounds and show various charming shapes as described herein. Although it is hard to completely understand the relationships between their morphologies and chemical structures, experimental and theoretical

approaches indicate several important factors such as:

a) moderate solubility into media,
b) intermolecular interaction moieties and their sterical position,
c) molecular shapes for highly ordered molecular packing,
d) molecular chirality.

Many reports also indicate a wide range of possible applications for these self-assembled nanofibers, from morphological applications such as preparation and utilization of replica of them to molecular level applications of specific molecular orientation. In this article, we introduced self-assembled nanofibers constructed mainly of relatively simple compounds, but oligomers and polymers such as cyclic polypeptide, cyclodextrin, and cyclic polysaccharide are also known to form self-assembled nanofibers [212].

It is prospected that self-assembling nano architectures including fibrillar aggregates have many potential applications because nature, especially human, is an excellent example of a hierarchical product of self-assembling molecules—there are so many excellent examples of hierarchical products of self-assembling molecules in nature itself, not the least of which is the human body. We sincerely hope that research on self-assembled nano architectures will be helpful in the development of molecularly precise materials and devices. The diversity of self-assembled nanofiber systems, including a large number of molecules, provides much opportunity to modify the chemical structures of self-assembling molecules. With the present rapid progress and expansion of this field, we feel a premonition that many applications will be found for nanofibers in the near future, including using combinations of morphologies and functions to provide suggestions for the origin of life.

GLOSSARY

α-helix One of the secondary structures of peptides, rod-like shape caused by intermolecular hydrogen bonding.

Amiloid fiber Fiber-like aggregate structures formed β-structure protein. These structures cause prion protein structure such as Alzheimer's disease or Bovine Spongiform Encephalopathy (BSE).

Atomic force microscope (AFM) Provide pictures of atoms on or in surfaces to measure the forces (at the atomic level) between a sharp probing tip (which is attached to a cantilever spring) and a sample surface.

β-sheet One of the secondary structures of peptides, its formed sheet-like shape is caused by intramolecular hydrogen bonding (antiparallel and parallel structure).

Bilayer membranes Amphiphiles self-organize in water to form molecular bilayers which assume the shape of globule, vesicle, lamella, fiber, and so on.

Carbon nanotube Fullerene-related structures that consist of graphene cylinders closed at either end with caps containing pentagonal rings.

Chiral/chirality Nonsuperimposable upon their mirror images and chirality is particularly important for molecules interacting within a biological environment, where many of the native molecules are chiral.

Circular dichroism (CD) The difference in absorption between left- and right-handed circulary polarized light.

Differencial scanning calorimetry (DSC) DSC measures the amount of energy (heat) absorbed or released by a sample as it is heated, cooled, or held at constant temperature. DSC also performs precise temperature measurements.

Hydrogen bonding Occurs where the partially positively charged hydrogen atom lies between partially negatively charged oxygen and nitrogen atoms.

Organogel Self-assembly of low molecular weight gelators to fiber-like structures, which entangle to form a three-dimensional network, immobilize organic fluids.

Peptide Two or more amino acids can be linked together by a dehydration synthesis to form a peptide. The characteristic chemical bond is called a peptide bond.

Supramolecular assemblies Infinite repeating structure comprised of several chemical species held together by intermolecular interactions and showing transcendent properties which are not observed in its constituent molecule alone.

Transmission electron microscopy (TEM) TEM allows to determine the internal structure of materials, either or biological or nonbiological origin used by a beam of electrons, to illuminate the sample.

ACKNOWLEDGMENTS

The authors deeply thank Ms. Yu Hamasaki, Mr. Tomohiro Shirosaki, and Mr. Takao Satoh for their capable assistance.

REFERENCES

1. J. Inglese, J. F. Glickman, W. Lorenz, M. G. Caron, and R. J. Lefkowitz, *J. Biol. Chem.* 267, 1422 (1992).
2. J. E. Tousa, W. Baehr, R. L. Martin, J. Hirsh, and W. L. Pak, *Cell* 40, 839 (1985).
3. A. F. Cowman, C. S. Zuker, and G. M. Rubin, *Cell* 44, 705 (1986).
4. C. S. Zuker, A. F. Cowman, and G. M. Rubin, *Cell* 40, 851 (1985).
5. S. S. Karnik, T. P. Sakmar, H. Chen, and H. Khorana, *Proc. Natl. Acad. Sci. U.S.A.* 85, 8459 (1988).
6. I. Nishie, K. Anzai, T. Yamamoto, and Y. Kirino, *J. Biol. Chem.* 265, 2488 (1990).
7. R. E. Dickerson, *Sci. Am.* 249, 94 (1983).
8. J. Kypr and M. Vorlickoba, *Gen. Phys. Biophys.* 4, 471 (1985).
9. E. Palecek, *Biol. Listy.* 53, 15 (1988).
10. M. Tsuboi, *Gendai Kagaku* 36, 360 (2001).
11. N. Sugimoto and S. Nakano, *Kagaku to Seibutsu* 39, 714 (2001).
12. E. H. Egelman, N. Francis, and D. J. DeRosier, *Nature* 298, 131 (1982).
13. M.-F. Carlier, D. Didry, I. Erk, J. Lepault, M. L. V. Troys, J. Vandekerckhove, I. Perelroizen, H. Yin, Y. Doi, and D. Pantaloni, *J. Biol. Chem.* 271, 9231 (1996).
14. B. J. Pope, S. M. Gonsior, S. Yeoh, A. McGough, and A. G. Weeds, *J. Mol. Biol.* 298, 649 (2000).
15. T. Ohno, *Saibo* 8, 170 (1976).
16. P. J. Butler, *J. Mol. Biol.* 72, 25 (1972).
17. P. J. Butler and J. T. Finch, *J. Mol. Biol.* 78, 637 (1973).
18. T. Ohno, T. Okada, Y. Nonomura, and H. Inoue, *J. Biochem.* 77, 313 (1975).
19. K. Raghavendra, J. A. Kelly, L. Khairallah, and T. M. Schuster, *Biochemistry* 27, 7583 (1988).
20. T. Kunitake, Y. Okahata, S. Shimomura, S. Yasunami, and K. Takarabe, *J. Am. Chem. Soc.* 103, 5401 (1981).

21. K. Yamada, H. Ihara, T. Ide, T. Fukumoto, and C. Hirayama, *Chem. Lett.* 1713 (1984).
22. H. Ihara, T. Fukumoto, C. Hirayama, and K. Yamada, *Polym. Commun.* 27, 282 (1986).
23. T. Kunitake and N. Yamada, *J. Chem. Soc., Chem. Commun.* 655 (1986).
24. H. Ihara, T. Fukumoto, C. Hirayama, and K. Yamada, *J. Chem. Soc. Jpn.* 543 (1987).
25. J. H. Georger, A. Shingh, R. R. Price, J. M. Schnur, P. Yager, and P. E. Schoen, *J. Am. Chem. Soc.* 109, 6169 (1987).
26. I. Cho and J. G. Park, *Chem. Lett.* 977 (1987).
27. J.-H. Fuhrhop, P. Schnieder, E. Boekema, and W. Helfrich, *J. Am. Chem. Soc.* 110, 2861 (1988).
28. H. Yanagawa, Y. Ogawa, H. Furuta, and K. Tsuno, *J. Am. Chem. Soc.* 111, 4567 (1989).
29. N. Kimizuka, H. Ohira, M. Tanaka, and T. Kunitake, *Chem. Lett.* 29 (1990).
30. H. Ihara, M. Yamaguchi, M. Takafuji, H. Hachisako, C. Hirayama, and K. Yamada, *J. Chem. Soc. Jpn.* 1047 (1990).
31. H. Ihara, K. Yoshikai, M. Takafuji, C. Hirayama, and K. Yamada, *Jpn. J. Polym. Sci. Tech.* 48, 377 (1991).
32. H. Ihara, M. Takafuji, C. Hirayama, and D. F. O'Brien, *Langmuir* 8, 1548 (1992).
33. T. Kunitake and Y. Okahata, *J. Am. Chem. Soc.* 99, 3860 (1977).
34. R. Jetter and M. Riederer, *Planta* 195, 257 (1994).
35. M. Lohmeyer and P. Workman, *Biochem. Pharmacol.* 819, 44 (1992).
36. S. Iijima, *Nature* 354, 56 (1991).
37. S. Iijima, T. Ichihara, and Y. Ando, *Nature* 356, 774 (1992).
38. J. Han, M. P. Anantram, R. F. Jaffe, J. Kong, and H. Dai, *Phys. Rev. B* 57, 14983 (1998).
39. D. S. Bethune, *Physica B* 323, 90 (2002).
40. S. Iijima and T. Ichihashi, *Nature* 363, 603 (1993).
41. D. S. Bethune, C. H. Kiang, M. S. de Vries, G. Gorman, R. Savoy, J. Vanquez, and R. Beyers, *Nature* 363, 605 (1993).
42. N. Nakashima, A. Asakuma, J.-M. Kim, and T. Kunitake, *Chem. Lett.* 1709 (1984).
43. N. Nakashima, A. Asakuma, and T. Kunitake, *J. Am. Chem. Soc.* 107, 509 (1985).
44. N. Hamada, S. Sawada, and A. Oshiyama, *Phys. Rev. Lett.* 68, 1579 (1992).
45. J. W. Mintmire, B. I. Dunlap, and C. T. White, *Phys. Rev. Lett.* 68, 631 (1992).
46. R. Saito, M. Fujita, G. Dresselhaus, and M. S. Dresselhaus, *Phys. Rev. B* 46, 1804 (1992).
47. R. Saito, M. Fujita, G. Dresselhaus, and M. S. Dresselhaus, *Appl. Phys. Lett.* 60, 2204 (1992).
48. K. Tanaka, K. Okahara, M. Okada, and T. Yamabe, *Chem. Phys. Lett.* 191, 469 (1992).
49. H. Ajiki and T. Ando, *J. Phys. Soc. Jpn.* 62, 1255 (1993).
50. J. E. Fischer, H. Dai, A. Thess, R. Ree, N. M. Hanjani, D. L. Dehaas, and R. E. Smalley, *Phys. Rev. B* 55, R 4921 (1997).
51. M. Bockrath, D. H. Cobden, P. L. McEuen, N. G. Chopra, A. Zettl, A. Thess, and R. E. Smalley, *Science* 275, 1922 (1997).
52. S. J. Tans, M. H. Devoret, H. Dai, A. Thess, R. E. Smalley, L. J. Geerlings, and C. Dekker, *Nature* 386, 474 (1997).
53. D. H. Cobden, M. Bockrath, P. L. McEuen, A. G. Rinzler, and R. E. Smalley, *Phys. Rev. Lett.* 81, 681 (1998).
54. S. J. Tans, A. R. M. Verschueren, and C. Dekker, *Nature* 393, 49 (1998).
55. B. W Smith and D. E. Luzzi, *Chem. Phys. Lett.* 321, 169 (2000).
56. B. W Smith, M. Monthioux, and D. E. Luzzi, *Chem. Phys. Lett.* 315, 31 (1999).
57. S. Iijima, *Physica B* 323, 1 (2002).
58. T. Shimizu, *Macromol. Rapid Commun.* 23, 311 (2002).
59. A. C. Dillon, K. M. Jones, T. A. Bekkedahi, C. H. Kiang, D. S. Bethune, and M. J. Heben, *Nature* 386, 377 (1997).
60. P. Chen, X. Wu, J. Lin, and K. L. Tan, *Science* 285, 91 (1999).
61. H. Dai, E. W. Wang, and C. M. Lieber, *Nature* 384, 147 (1996).
62. H. Nishijima, S. Kamo, S. Akita, Y. Nakayama, K. I. Hohmura, S. H. Yoshimura, and K. Takeyasu, *Appl. Phys. Lett.* 74, 4061 (1999).
63. K. Hanabusa, T. Miki, Y. Taguchi, T. Koyama, and H. Shirai, *J. Chem. Soc., Chem. Commun.* 1382 (1993).
64. C. Gregolire, S. Marco, J. Thimonier, L. Duplan, E. Jaurine, J.-P. Cheuvin, B. Michael, V. Peyort, and J.-M. Verdier, *EMBO. J.* 20, 3313 (2001).
65. J. H. Jung and S. Shinkai, *Journal of Inclusion Phenomena and Macrocyclic Chemistry* 41, 53 (2001).
66. S. Mabrey and J. M. Sturtevant, *Proc. Natl. Acad. Sci. U.S.A.* 73, 3862 (1976).
67. T. Kajiyama, A. Kumano, M. Takayanagi, Y. Okahata, and T. Kunitake, *Chem. Lett.* 645 (1979).
68. Y. Okahata and T. Kunitake, *Ber. Bunsenges. Phys. Chem.* 84, 550 (1980).
69. T. Kunitake, H. Ihara, and Y. Okahata, *J. Am. Chem. Soc.* 105, 6070 (1983).
70. H. Ihara, H. Hachisako, C. Hirayama, and K. Yamada, *J. Chem. Soc. Chem. Commun.* 1244 (1992).
71. T. Kimura and S. Shinkai, *Chem. Lett.* 1035 (1998).
72. T. Kato, G. Kondo, and K. Hanabusa, *Chem. Lett.* 193 (1998).
73. H. Ihara, M. Yoshitake, M. Takafuji, T. Yamada, T. Sagawa, C. Hirayama, and H. Hachisako, *Liq. Cryst.* 26, 1021 (1999).
74. T. Kunitake, N. Nakashima, M. Shimomura, Y. Okahata, K. Kano, and T. Ogawa, *J. Am. Chem. Soc.* 102, 6642 (1980).
75. M. Shimomura and T. Kunitake, *Chem. Lett.* 1001 (1981).
76. H. Ihara, H. Hachisako, C. Hirayama, and K. Yamada, *Liq. Cryst.* 2, 215 (1987).
77. J. E. Sohna and F. Fages, *Chem. Commun.* 327 (1997).
78. N. Amanokura, K. Yasumasa, and S. Shinkai, *J. Chem. Soc. Perkin Trans.* 2 1995 (1999).
79. K. Kano, A. Romero, B. Djermouni, H. J. Ache, and J. H. Fendler, *J. Am. Chem. Soc.* 101, 4030 (1979).
80. T. Sagawa, S. Fukugawa, T. Yamada, and H. Ihara, *Langmuir* 18, 7223 (2002).
81. T. Nagamura, S. Mihara, Y. Okahata, T. Kunitake, and T. Matsuo, *Ber. Bunsenges. Phys. Chem.* 82, 1093 (1978).
82. M. Shimomura, R. Ando, and T. Kunitake, *Ber. Bunsenges. Phys. Chem.* 87, 1134 (1983).
83. H. Hachisako, H. Ihara, T. Kamiya, C. Hirayama, and K. Yamada, *Chem. Commun.* 19 (1997).
84. J. M. Schnur, B. R. Ratna, J. V. Seliger, A. Singh, G. Jyothi, and K. R. K. Easwaran, *Science* 264, 945 (1994).
85. N. Nakashima, H. Fukushima, and T. Kunitake, *Chem. Lett.* 1207 (1981).
86. N. Nakashima and T. Kunitake, *J. Am. Chem. Soc.* 104, 4261 (1982).
87. T. Arimura, M. Shibata, H. Ihara, and C. Hirayama, *Anal. Sci.* 9, 401 (1993).
88. A. D. Bungham, M. M. Standish, and J. C. Watkins, *J. Mol. Biol.* 13, 238 (1965).
89. K. Yamada, H. Shosenji, H. Ihara, and O. Hotta, *Chem. Lett.* 43 (1983).
90. T. Kunitake, N. Kimizuka, N. Higashi, and N. Nakashima, *J. Am. Chem. Soc.* 106, 1978 (1984).
91. J.-H. Fuhrhop, P. Schnieder, J. Rosenberg, and R. Boekema, *J. Am. Chem. Soc.* 109, 3387 (1987).
92. J.-H. Fuhrhop, S. Svenson, C. Boettcher, E. Rossler, and H.-M. Vieth, *J. Am. Chem. Soc.* 112, 4307 (1990).
93. J. Koning, C. Boettcher, H. Winkler, E. Zeitler, Y. Talmon, and J.-H. Fuhrhop, *J. Am. Chem. Soc.* 115, 693 (1993).
94. T. Imae, Y. Takahashi, and H. Muramatsu, *J. Am. Chem. Soc.* 114, 3414 (1992).

95. R. Oda, I. Huc, M. Schmutz, S. J. Candau, and F. C. MacKintosh, *Nature* 399, 566 (1999).
96. R. Oda, I. Huc, and S. J. Candau, *Angew. Chem. Int. Ed.* 37, 2689 (1998).
97. W. Helfrich and W. Harbich, *Chem. Scr.* 25, 32 (1985).
98. W. Helfrich, *J. Chem. Phys.* 85, 1085 (1986).
99. W. Helfrich and J. Prost, *Phys. Rev. A* 38, 3065 (1988).
100. W. Helfrich, *Langmuir* 7, 567 (1991).
101. J. V. Selinger, M. S. Spector, and J. M. Schnur, *J. Phys. Chem. B* 105, 1757 (2001).
102. N. Nandi and B. Bagchi, *J. Am. Chem. Soc.* 118, 11208 (1996).
103. T. Kunitake, N. Nakashima, and M. Kunitake, *Macromolecules* 22, 3544 (1989).
104. S. Zhang and M. Altman, *Reactive & Functional Polymers* 41, 91 (1999).
105. M. R. Caplan, E. M. Schwartzfarb, S. Zhang, R. D. Kamm, and D. A. Lauenburger, *Biomaterials* 23, 219 (2002).
106. Y.-C. Yu, P. Berndt, M. Tirrell, and G. B. Fields, *J. Am. Chem. Soc.* 118, 12515 (1996).
107. M. Altman, P. Lee, A. Rich, and S. Zhang, *Protein Science* 9, 1095 (2000).
108. M. R. Caplan, P. N. Moore, S. Zhang, R. D. Kamm, and D. A. Lauffenburger, *Biomacromolecules* 1, 627 (2000).
109. L. A. Scrocchi, Y. Chen, S. Waschuk, F. Wang, S. Cheung, A. A. Darabie, J. McLaurin, and P. E. Fraser, *J. Mol. Biol.* 318, 697 (2002).
110. T. Kowalewski and D. M. Holtzman, *Proc. Natl. Acad. Sci. U.S.A.* 96, 3688 (1999).
111. R. Jayakumar, M. Murugesan, C. Asokan, and M. A. Scibioh, *Langmuir* 16, 1489 (2000).
112. H. A. Lashuel, S. R. LaBrenz, L. Woo, L. C. Serpell, and J. W. Kelly, *J. Am. Chem. Soc.* 122, 5262 (2000).
113. K. Tenidis, M. Waldner, J. Bernhagen, W. Fiscle, M. Bermann, M. Weþer, M.-L. Merkle, W. Voelte, H. Brunner, and A. Kapurniotu, *J. Mol. Biol.* 295, 1055 (2000).
114. M. M. Martinez-Senac, J. Villalain, and J. C. Gomez-Fernandez, *Eur. J. Biochem.* 265, 744 (1999).
115. T. Sakurai, M. Koga, M. Takafuji, and H. Ihara, *Chem. Lett.* 152 (2003).
116. M. S. Specter, J. V. Selinger, A. Singh, J. M. Rodriguez, R. R. Price, and J. M. Schnur, *Langmuir* 14, 3493 (1998).
117. M. Hatano, M. Yoneyama, Y. Sato, and Y. Kawamura, *Biopolymers* 12, 2423 (1973).
118. H. Ihara, M. Shibata, and C. Hirayama, *Chem. Lett.* 1731 (1992).
119. M. Shibata, H. Ihara, and C. Hirayama, *Polymer* 34, 1106 (1993).
120. Y. Osada and A. R. Khokhlov, "Polymer Gels and Networks," Marcel Dekker, Inc., New York (2001).
121. J. P. Cohen Addad, "Physical Properties of Polymeric Gels," John Wiley & Sons, Inc., Hoboken, NJ (1996).
122. K. Almdal, J. Dyre, S. Hvidt, and O. Kramer, *Polym. Gels Networks* 1, 5 (1993).
123. P. Terech and R. Weiss, *Chem. Rev.* 97, 3133 (1997).
124. Y.-C. Lin and R. G. Weiss, *Macromolecules* 20, 414 (1987).
125. T. Brotin, R. Utermohlen, F. Fages, H. Bouas-Laurent, and J. P. Desvergne, *J. Chem. Soc., Chem Commun.* 416 (1991).
126. Y. Ishikawa, H. Kuwahara, and T. Kunitake, *J. Am. Chem. Soc.* 111, 8530 (1989).
127. N. Ide, T. Fukuda, and T. Miyamoto, *Bull. Chem. Soc. Jpn.* 68, 3423 (1995).
128. T. Tachibana and H. Kambara, *J. Am. Chem. Soc.* 87, 3016 (1965).
129. T. Tachibana, T. Mori, and K. Mori, *Bull. Chem. Soc. Jpn.* 53, 1741 (1980).
130. A. T. Polishuk, *J. Am. Soc. Lubn. Eng.* 22, 133 (1977).
131. P. Terech, A Coutin, and A. M. Giround-Godquin, *J. Phys. Chem. B* 101, 6810 (1994).
132. K. Hanabusa, K. Okui, K. Karaki, T. Koyama, and H. Shirai, *J. Chem. Soc., Chem. Commun.* 1371 (1992).
133. K. Hanabusa, K. Hiratsuka, M. Kimura, and H. Shirai, *Chem. Mater.* 11, 649 (1999).
134. K. Hanabusa, J. Tange, Y. Taguchi, T. Koyama, and H. Shirai, *J. Chem. Soc., Chem. Commun.* 390 (1993).
135. K. Hanabusa, M. Yamada, M. Kimura, and H. Shirai, *Angew. Chem. Int. Ed. Engl.* 35, 1949 (1996).
136. K. Hanabusa, K. Shimura, K. Hirose, M. Kimura, and H. Shirai, *Chem. Lett.* 885 (1996).
137. P. Thiyagarajan, F. Zeng, C. Y. Ku, and S. C. Zimmermanb, *J. Mater. Chem.* 7, 1221 (1997).
138. R. J. H. Hafkamp, B. P. A. Kokke, I. M. Danke, H. P. M. Geurts, A. E. Rowan, M. C. Feiters, and R. J. M. Nolte, *Chem. Commun.* 545 (1997).
139. A. Friggeri, O. Gronwald, K. J. C. Bommel, S. Shinkai, and D. N. Reinhoudt, *Chem. Commun.* 2434 (2001).
140. O. Gronwald and S. Shinkai, *Chem. Eur. J.* 7, 4328 (2001).
141. O. Gronwald, E. Snip, and S. Shinkai, *Current Opinion in Colloid & Interface Science* 7, 148 (2002).
142. I. Furman and R. G. Weiss, *Langmuir* 9, 2084 (1993).
143. R. Mukkamala and R. G. Weiss, *J. Chem. Soc., Chem. Commun.* 375 (1995).
144. R. Mukkamala and R. G. Weiss, *Langmuir* 12, 1474 (1996).
145. D. J. Abdallah and R. G. Weiss, *Adv. Mater.* 12, 1237 (2000).
146. L. Lu, D. L. Cocker, R. E. Bachman, and R. G. Weiss, *Langmuir* 16, 20 (2000).
147. U. Maitra, P. V. Kumar, N. Chandra, L. J. D'Souza, M. D. Prasanna, and A. R. Raju, *Chem. Commun.* 595 (1999).
148. F. Placin, M. Colomes, and J.-P. Desvergne, *Tetrahedron Lett.* 38, 2665 (1997).
149. J.-L. Pozzo, G. M. Clavier, and J.-P Desvergne, *J. Mater. Chem.* 8, 2575 (1998).
150. G. M. Clavier, J.-F. Brugger, H. Bouas-Laurent, and J.-L. Pozzo, *J. Chem. Soc., Perkin Trans.* 2 2527 (1998).
151. P. Terech, C. Chachaty, J. Gaillard, and A. M. Giroud-Godquin, *J. Phys. Fr.* 48, 663 (1987).
152. A. M. Godquin-Giroud, *J. Phys. Lett.* 45, L-387 (1984).
153. A. M. Godquin-Giroud, M. M. Gauthier, G. Sigaud, F. Hardouin, and F. Achard, *Mol. Cryst. Liq. Cryst.* 132, 35 (1986).
154. A. M. Godquin-Giroud and J. C. Marchon, *J. Phys. Lett.* 45, L-681 (1984).
155. G. S. Attard and P. R. Cullum, *Liq. Cryst.* 8, 299 (1990).
156. H. Abied, D. Guillon, A. Skoulios, P. Weber, A. M. Godquin-Giroud, and J. C. Marchon, *Liq. Cryst.* 2, 269 (1987).
157. H. Ihara, K. Shudo, M. Takafuji, C. Hirayama, H. Hachisako, and K. Yamada, *Jpn. J. Polym. Sci. Technol.* 52, 606 (1995).
158. M. de Loos, J. van Esch, I. Stokroos, R. M. Kellogg, and B. L. Feringa, *J. Am. Chem. Soc.* 119, 12675 (1997).
159. M. Masuda, T. Honda, K. Yase, and T. Shimizu, *Macromolecules* 31, 9403 (1998).
160. M. Masuda, T. Honda, Y. Okada, K. Yase, and T. Shimizu, *Macromolecules* 33, 9233 (2000).
161. K. Hanabusa, Y. Maesaka, M. Suzuki, M. Kimura, and H. Shirai, *Chem. Lett.* 1168 (2000).
162. W. Gu, L. Lu, G. B. Chapman, and R. G. Weiss, *Chem. Commun.* 543 (1997).
163. M. Takafuji, A. Ishiodori, and H. Ihara, "Proc. Int. Symp. Bioorg. Chem.," 2002, Toronto, Canada.
164. Y. Ono, K. Nakashima, M. Sano, Y. Kanekiyo, K. Inoue, J. Hojo, and S. Shinkai, *Chem. Commun.* 1477 (1998).
165. Y. Ono, K. Nakashima, M. Sano, J. Hojo, and S. Shinkai, *Chem. Lett.* 1119 (1999).
166. J. H. Jung, Y. Ono, and S. Shinkai, *Langmuir* 16, 1643 (2000).
167. J. H. Jung, Y. Ono, and S. Shinkai, *J. Chem. Soc., Perkin Trans.* 2 1289 (1999).
168. J. H. Jung, Y. Ono, K. Sakurai, M. Sano, and S. Shinkai, *J. Am. Chem. Soc.* 122, 8648 (2000).

169. M. Takafuji, H. Ihara, C. Hirayama, H. Hachisako, and K. Yamada, *Liq. Cryst.* 18, 97 (1995).
170. H. Ihara, K. Shudo, H. Hachisako, K. Yamada, and C. Hirayama, *Liq. Cryst.* 20, 807 (1996).
171. M. Takafuji, T. Sakurai, T. Hashimoto, N. Kido, T. Yamada, T. Sagawa, H. Hachisako, and H. Ihara, *Chem. Lett.* 7223 (2002).
172. H. Ihara, T. Sakurai, T. Yamada, T. Hashimoto, M. Takafuji, T. Sagawa, and H. Hachisako, *Langmuir* 18, 7120 (2002).
173. T. Ishi-i, J. H. Jung, and S. Shinkai, *J. Mater. Chem.* 10, 2238 (2000).
174. T. Ishi-i, R. Iguchi, E. Snip, M. Ikeda, and S. Shinkai, *Langmuir* 17, 1825 (2001).
175. K. Murata, M. Aoki, T. Nishi, A. Ikeda, and S. Shinkai, *J. Chem. Soc., Chem. Commun.* 1715 (1991).
176. K. Murata, M. Aoki, T. Suzuki, T. Harada, H. Kawabata, T. Komori, F. Ohseto, K. Ueda, and S. Shinkai, *J. Am. Chem. Soc.* 116, 6664 (1994).
177. S. Shinkai and K. Murata, *J. Mater. Chem.* 8, 485 (1998).
178. A. Halperin and S. Alexander, *Macromolecules* 22, 2403 (1989).
179. Z. Zhou, B. Chu, and D. G. Peiffer, *Macromolecules* 26, 1876 (1993).
180. Z. Tuzer and P. Kratochvil, *Surface Colloid Sci.* 15, 1 (1993).
181. R. Nagarajan and K. Ganesh, *J. Chem. Phys.* 90, 5843 (1989).
182. F. S. Bates and G. H. Fredrickson, *Ann. Rev. Phys. Chem.* 15, 584 (1990).
183. F. S. Bates, *Science* 251, 898 (1991).
184. E. L. Thomas, D. M. Anderson, C. S. Henkee, and D. Hoffman, *Nature* 334, 598 (1988).
185. S. Sakurai, *Trends Polym. Sci.* 3, 90 (1995).
186. L. Qi, H. Cölfen, and M. Antonietti, *Angew. Chem. Int. Ed.* 39, 604 (2000).
187. K. de Moel, G. O. R. Ekenstein, H. Nijland, E. Polushkin, and G. Brinke, *Chem. Mater.* 13, 4580 (2001).
188. H. Fong and D. H. Reneker, *J. Polym. Sci. B* 37, 3488 (1999).
189. G. Liu, J. Ding, L. Qiao, A. Guo, B. P. Dymov, J. T. Gleeson, T. Hashimoto, and K. Saijo, *Chem. Eur. J.* 5, 2740 (1999).
190. G. Liu, L. Qiao, and A. Guo, *Macromolecules* 29, 5508 (1996).
191. T. Fujiwara and Y. Kimura, *Macromol. Biosci.* 2, 11 (2002).
192. X. Yang, G. Liu, F. Liu, B. Z. Tang, H. Peng, A. B. Pakhomov, and C. Y. Wong, *Angew. Chem. Int. Ed.* 40, 3593 (2001).
193. K. L. Wooley, *J. Polym. Sci., Polym. Chem.* 38, 1397 (2000).
194. G. Che, B. B. Lakshmi, C. R. Martin, and E. R. Fisher, *Chem. Mater.* 10, 260 (1998).
195. M. Gao, S. Huang, L. Dai, G. Wallace, R. Gao, and Z. Wang, *Angew. Chem.* 112, 3810 (2000).
196. Z. Liu, Y. Sakamoto, T. Ohsuna, K. Hiraga, O. Terasaki, C. H. Ko, H. J. Shin, and R. Ryoo, *Angew. Chem.* 112, 3237 (2000).
197. A. G. MacDiarmid, W. E. Jones, I. D. Norris, J. Gao, A. T. Jhonson, N. J. Pinto, J. Hone, B. Han, F. K. Ko, H. Okazaki, and M. Llaguno, *Synthetic Metals* 119, 27 (2001).
198. B. Yu and H. Li, *Materials Science and Engineering* A325, 215 (2002).
199. L. Feng, S. Li, H. Li, J. Zhai, Y. Song, L. Jiang, and D. Zhu, *Angew. Chem. Int. Ed.* 41, 1221 (2002).
200. J. Bico, C. Marzolin, and D. Quéré, *Europhys. Lett.* 47, 220 (1999).
201. S. Shibuichi, T. Yamamoto, T. Onda, and K. Tsujii, *J. Colloid Interface Sci.* 208, 287 (1998).
202. A. F. Thüemann, *Langmuir* 16, 824 (2000).
203. T. Nishino, M. Meguro, K. Nakamae, and M. Matsushita, *Langmuir* 15, 4321 (1999).
204. P. Kovacic and M. B. Jones, *Chem. Rev.* 87, 357 (1987).
205. G. Grem, G. Leditzky, B. Ullrich, and G. Lesising, *Adv. Mater.* 4, 36 (1992).
206. P. Kovacic and A. Kyriakis, *J. Am. Chem. Soc.* 85, 454 (1963).
207. A. Formhals, U.S. Patent No. 1 975, 504 (1944).
208. J. Doshi and D. H. Reneker, *J. Electrost.* 35 (1999).
209. P. W. Gibson, H. L. Schreuder-Gibson, and D. Riven, *AIChE J.* 45 (1999).
210. D. H. Reneker, A. L. Yarin, H. Fong, and S. Koombhongse, *J. Appl. Phys.* 87, 4531 (2000).
211. I. D. Norris, M. M. Shaker, F. K. Ko, and A. G. MacDiarmid, *Synthetic Metals* 114, 109 (2000).
212. D. T. Bong, T. D. Clark, J. R. Granju, and M. R. Ghadiri, *Angew. Chem. Int. Ed.* 40, 988 (2001).
213. H. Hachisako, H. Nakayama, and H. Ihara, *Chem. Lett.* 1165 (1999).
214. J. H. Esch and B. L. Feringa, *Angew. Chem. Int. Ed.* 39, 2263 (2000).
215. K. Yoza, Y. Ono, K. Yoshihira, T. Akao, H. Shinmori, M. Takeuchi, S. Shinkai, and D. N. Reinhoudt, *J. Chem. Soc., Chem. Commun.* 907 (1998).
216. M. Smith and D. E. Katsoulis, *J. Mater. Chem.* 5, 1899 (1995).
217. Y. Ishikawa, H. Kuwabara, and T. Kunitake, *J. Am. Chem. Soc.* 116, 5579 (1994).
218. T. Kimura, T. Yamashita, K. Koumoto, and S. Shinkai, *Tetrahedron Lett.* 40, 6631 (1999).
219. N. Mizoshita, T. Kutsuna, K. Hanabusa, and T. Kato, *Chem. Commun.* 781 (1997).
220. X. Luo, C. Li, and Y. Liang, *Chem. Commun.* 2091 (2000).
221. R. Wang, C. Geiger, L. Chen, B. Swanson, and D. G. Whitten, *J. Am. Chem. Soc.* 122, 2399 (2000).
222. X. Luo, B. Liu, and Y. Liang, *Chem. Commun.* 1556 (2001).
223. S. Bhattacharya and Y. Krishnan-Ghosh, *Chem. Commun.* 185 (2001).
224. H. M. Willemen, T. Vermonden, A. T. M. Marcelis, and E. J. R. Sudholter, *Langmuir* 18, 7102 (2002).
225. S. A. Ahmed, X. Sallenave, F. Fages, G. Mieden-Gundert, W. M. Muller, F. Vogtle, and J.-L. Pozzo, *Langmuir* 18, 7096 (2002).
226. H. Ihara, K. Shudo, M. Takafuji, C. Hirayama, and K. Yamada, *J. Chem. Soc., Chem. Commun.* 1244 (1992).
227. M. de Loos, J. H. Esch, I. Stokroos, R. M. Kellogg, and B. L. Feringa, *J. Am. Chem. Soc.* 119, 12675 (1997).
228. H. Hachisako, T. Murata, and H. Ihara, *J. Chem. Soc., Perkin Trans.* 2, 2569 (1999).
229. H. Ihara, M. Yoshitake, M. Takafuji, T. Yamada, T. Sagawa, and C. Hirayama, *Liq. Cryst.* 26, 1021 (1999).
230. F. S. Schoonbeek, J. H. Esch, B. Wegewijs, D. B. A. Rep, M. P. de Haas, T. M. Klapwijk, R. M. Kellogg, and B. L. Feringa, *Angew. Chem. Int. Ed.* 38, 1393 (1999).
231. K. Ariga, J. Kikuchi, M. Naito, E. Koyama, and N. Yamada, *Langmuir* 16, 4929 (2000).
232. M. Kimura, T. Kitamura, T. Muto, K. Hanabusa, H. Shirai, and N. Kobayashi, *Chem. Lett.* 1088 (2000).
233. M. Suzuki and C. C. Waraksa, *Chem. Commun.* 2012 (2001).
234. K. Tomioka, T. Sumiyoshi, S. Narui, Y. Nagaoka, A. Iida, Y. Miwa, T. Taga, M. Nakano, and T. Handa, *J. Am. Chem. Soc.* 123, 11817 (2001).
235. M. de. Loos, J. H. Esch, R. M. Kellogg, and B. L. Feringa, *Angew. Chem. Int. Ed.* 40, 613 (2001).
236. G. Wang and A. D. Hamilton, *Chem. Eur. J.* 8, 1954 (2002).
237. S. Laan, B. L. Feringa, R. M. Kellogg, and J. H. Esch, *Langmuir* 18, 7136 (2002).
238. C. F. Nostrum, S. J. Picken, A.-J. Schouten, and R. J. M. Nolte, *J. Am. Chem. Soc.* 117, 9957 (1995).
239. U. Beginn, G. Zipp, and M. Moler, *Adv. Mater.* 12, 510 (2000).
240. J. Loisea, M. Lescanne, A. Colin, F. Fages, J.-B. Verlhac, and J.-M. Vincent, *Tetrahedron* 58, 4049 (2002).
241. Y. Lin and R. G. Weiss, *Macromolecules* 2, 414 (1987).
242. H. J. Tian, K. Inoue, K. Yoza, T. Ishi-I, and S. Shinkai, *Chem. Lett.* 871 (1998).

243. J. H. Jung, H. Kobayashi, K. J. C. Bommel, S. Shinkai, and T. Shimizu, *Chem. Mater.* 14, 1445 (2002).
244. J. Massey, K. N. Power, I. Manners, and M. A. Winnik, *J. Am. Chem. Soc.* 120, 9533 (1998).
245. A. Ajayaghosh and S. J. George, *J. Am. Chem. Soc.* 123, 5148 (2001).
246. Y. Tsabba, D. M. Rein, and Y. Cohen, *J. Polym. Sci. B.* 40, 1087 (2002).
247. N. Amanokura, Y. Kanekiyo, S. Shinkai, and D. N. Reinhoudt, *J. Chem. Soc., Perkin Trans.* 2 1995 (1999).
248. M. S. Vollmer, T. D. Clark, C. Steinem, and M. R. Ghadiri, *Angew. Chem. Int. Ed.* 38, 1598 (1999).
249. K. Hanabusa, M. Matsumoto, M. Kimura, A. Kakehi, and H. Shirai, *J. Colloid Interface. Sci.* 224 (2000).
250. A. Carre, P. L. Grel, and M. B. Floch, *Tetrahedron Lett.* 42, 1887 (2001).
251. A. Aggeli, I. A. Nyrkova, M. Bell, R. Harding, L. Carrick, T. C. B. McLeish, A. N. Semenov, and N. Boden, *Proc. Natl. Acad. Sci. U.S.A.* 98, 11857 (2001).
252. J. H. Esch, R. M. Kellogg, and B. L. Feringa, *Tetrahedron Lett.* 38, 281 (1997).
253. K. Inoue, T. Ono, Y. Kanekiyo, T. Ishi-i, K. Yoshihara, and S. Shinkai, *J. Org. Chem.* 64, 2933 (1999).
254. F. S. Schoonbeek, J. H. Esch, R. Hulst, R. M. Kellogg, and B. L. Feringa, *Chem. Eur. J.* 6, 2633 (2000).
255. M. de Loos, A. G. J. Ligtenbarg, J. H. Esch, H. Kooijman, A. L. Spec, R. Hage, R. M. Kellogg, and B. L. Feringa, *Eur. J. Org. Chem.* 3675 (2000).
256. H. M. Willemen, T. Vermonden, A. T. M. Marcelis, and E. J. R. Sudholter, *Eur. J. Org. Chem.* 2329 (2001).
257. M. Kolbel and F. M. Menger, *Chem. Commun.* 275 (2001).